Am J Physiol Renal Physiol 318: F402–F421, 2020.
First published December 16, 2019; doi:10.1152/ajprenal.00481.2019.

RESEARCH ARTICLE

NBCe1-A is required for the renal ammonia and K^+ response to hypokalemia

Hyun-Wook Lee,[1] Autumn N. Harris,[1] Michael F. Romero,[2] Paul A. Welling,[3] Charles S. Wingo,[1,4] Jill W. Verlander,[1] and I. David Weiner[1,4]

[1]*Division of Nephrology, Hypertension and Renal Transplantation, University of Florida College of Medicine, Gainesville, Florida;* [2]*Department of Physiology and Biomedical Engineering, Mayo Clinic, Rochester, Minnesota;* [3]*Nephrology Division, Departments of Medicine and Physiology, Johns Hopkins Medical School, Baltimore, Maryland; and* [4]*Nephrology and Hypertension Section, Gainesville Veterans Affairs Medical Center, Gainesville, Florida*

Submitted 10 October 2019; accepted in final form 12 December 2019

Lee HW, Harris AN, Romero MF, Welling PA, Wingo CS, Verlander JW, Weiner ID. NBCe1-A is required for the renal ammonia and K^+ response to hypokalemia. *Am J Physiol Renal Physiol* 318: F402–F421, 2020. First published December 16, 2019; doi:10.1152/ajprenal.00481.2019.—Hypokalemia increases ammonia excretion and decreases K^+ excretion. The present study examined the role of the proximal tubule protein NBCe1-A in these responses. We studied mice with Na^+-bicarbonate cotransporter electrogenic, isoform 1, splice variant A (NBCe1-A) deletion [knockout (KO) mice] and their wild-type (WT) littermates were provided either K^+ control or K^+-free diet. We also used tissue sections to determine the effect of extracellular ammonia on NaCl cotransporter (NCC) phosphorylation. The K^+-free diet significantly increased proximal tubule NBCe1-A and ammonia excretion in WT mice, and NBCe1-A deletion blunted the ammonia excretion response. NBCe1-A deletion inhibited the ammoniagenic/ammonia recycling enzyme response in the cortical proximal tubule (PT), where NBCe1-A is present in WT mice. In the outer medulla, where NBCe1-A is not present, the PT ammonia metabolism response was accentuated by NBCe1-A deletion. KO mice developed more severe hypokalemia and had greater urinary K^+ excretion during the K^+-free diet than did WT mice. This was associated with blunting of the hypokalemia-induced change in NCC phosphorylation. NBCe1-A KO mice have systemic metabolic acidosis, but experimentally induced metabolic acidosis did not alter NCC phosphorylation. Although KO mice have impaired ammonia metabolism, experiments in tissue sections showed that lack of ammonia does impair NCC phosphorylation. Finally, urinary aldosterone was greater in KO mice than in WT mice, but neither expression of epithelial Na^+ channel α-, β-, and γ-subunits nor of H^+-K^+-ATPase α_1- or α_2-subunits correlated with changes in urinary K^+. We conclude that NBCe1-A is critical for the effect of diet-induced hypokalemia to increase cortical proximal tubule ammonia generation and for the expected decrease in urinary K^+ excretion.

ammonia; potassium; proximal tubule

INTRODUCTION

Hypokalemia stimulates renal ammonia[1] metabolism despite the frequent simultaneous occurrence of metabolic alkalosis (18, 33, 65, 73). This is counterproductive from an acid-base homeostasis perspective, as increased ammonia excretion increases renal bicarbonate generation and can lead to further systemic alkalinization rather than to correction of the metabolic alkalosis that is often seen with hypokalemia. Moreover, the increased ammonia generation may contribute to extrarenal disease, such as precipitation of hyperammonemic encephalopathy in patients with underlying liver disease (79). Thus, understanding the mechanisms through which hypokalemia increases ammonia metabolism is important.

One recently identified mechanism regulating ammonia metabolism in other conditions involves the basolateral Na^+-bicarbonate cotransporter electrogenic, isoform 1, splice variant A (NBCe1-A). NBCe1-A is present in cortical proximal tubule segments, where it functions as the primary basolateral bicarbonate exit mechanism for filtered bicarbonate reabsorption and for proximal tubule bicarbonate that is generated during ammoniagenesis (1, 38, 56). Recent studies have shown that NBCe1-A also regulates both basal ammonia metabolism and the response to metabolic acidosis and that it does so by regulating expression of multiple proximal tubule proteins involved in ammonia generation (45). Whether it also regulates the response to hypokalemia has not been studied previously.

The purpose of the present study was to determine the role of NBCe1-A in the renal response to diet-induced hypokalemia. First, we evaluated the effect of diet-induced hypokalemia on NBCe1-A expression. Next, we determined the effect of NBCe1-A deletion on urine and serum electrolyte response to a K^+-free diet. We then identified which proteins involved in ammonia metabolism exhibited altered expression in response to hypokalemia as a result of NBCe1-A deletion. Because NBCe1-A deletion also altered the K^+ response to hypokalemia, we determined the effect of NBCe1-A deletion on NaCl cotransporter (NCC) phosphorylation, which has a key role in regulating renal K^+ homeostasis. Our results showed that NBCe1-A has an essential role in both the renal ammonia and K^+ homeostatic responses to hypokalemia through altered expression of key proteins involved both in ammonia metabolism in the proximal tubule and in K^+ homeostasis in the distal nephron.

METHODS

Animals. We used mice with NBCe1-A-specific deletion (45). All breeding involved heterozygous dams with heterozygous sires, and age- and sex-matched wild-type (WT) and knockout (KO) offspring were used in these experiments. We genotyped mice using DNA

Address for reprint requests and other correspondence: I. D. Weiner, Div. of Nephrology, Hypertension and Transplantation, Univ. of Florida College of Medicine, PO Box 100224, Gainesville, FL 32610 (e-mail: david.weiner@medicine.ufl.edu).

[1] Ammonia is present in two molecular forms, NH_3 and NH_4^+, which are in equilibrium with each other. In this report, we use the term "ammonia" to refer to the combination of both molecular forms. When referring to a specific molecular form, we state specifically either "NH_3" or "NH_4^+."

extracted from tail clip samples as detailed above (45). The Institutional Animal Care and Use Committees of the University of Florida and the North Florida/South Georgia Veterans Health System approved all animal experiments. All mice were on the C57BL/6 background strain.

Antibodies. All antibodies used have been previously described. The specific antibodies, sources, and dilutions used are shown in Table 1.

Metabolic cage experiments. Mice were housed in metabolic cages throughout the duration of the experiment, and daily 24-h urine collections were made as previously described (5, 6, 41–43, 46–48). Daily food intake was measured. Urine pH and volume were measured in each 24-h collection, and urine was then frozen for further analysis at a later time.

Dietary maneuvers. Hypokalemia was induced by feeding mice a K^+ control diet (TD.88238, Harlan Teklad, Madison, WI) for 2 days followed by a nominally K^+-free diet (TD.88239, Harlan Teklad) for 4 days. We obtained powdered food and mixed it with H_2O in a ratio of 6 g of food to 1 mL of H_2O to form a semisolid diet. Normokalemic mice were provided the K^+ control diet in an identical manner.

Plasma analyses. Blood was obtained by cannulation of the aorta, drawn into a heparinized syringe, and immediately analyzed for Na^+, K^+, and bicarbonate concentrations using a Siemens Microanalytic Blood Gas Analyzer (RAPIDLab 348 Analyzer, Siemens).

Urinary analysis. Urine ammonia was measured using a modification of a commercially available kit (no. A7553, Pointe Scientific, Canton, MI) as previously described (5, 36). Urine pH was measured using a micro-pH electrode (ROSS Semi-Micro pH, Orion 8115BN; Thermo Scientific). Urine aldosterone was measured using an Aldosterone ELISA Kit (no. 501090, Cayman Chemical, Ann Arbor, MI) according to the manufacturer's instructions.

Tissue handling. Mice were anesthetized with inhalant isoflurane anesthesia, and tissues were preserved by in vivo cardiac perfusion with PBS (pH 7.4) containing 6,000 U/L Na-heparin and 120 mg/L Lidocaine followed by periodate-lysine-2% paraformaldehyde (PLP) fixation. Kidney tissue was processed in polyester wax and sectioned as previously described (5, 6, 41–44, 46–48). Kidney proteins and mRNA for immunoblot analysis and real-time RT-PCR were obtained using previously described techniques (5, 6, 41–44, 46–48).

Immunohistochemistry. Immunolocalization was accomplished using immunoperoxidase procedures routinely used in our laboratory (29, 30, 40, 43, 48, 55). Briefly, sections were deparaffinized in xylene and ethanol, rehydrated, and then rinsed in PBS. Antigen retrieval was accomplished by immersing slides in Trilogy (Cell Marque, Rocklin, CA) at 96°C for 1 h. Endogenous peroxidase activity was blocked by incubation of the sections in 3% H_2O_2 in methanol for 45 min. After being washed in PBS, sections were treated with 0.5% Triton X-100 in PBS for 15 min. Sections then underwent several washes in PBS containing 1% BSA, 0.05% saponin, and 0.2% gelatin followed by incubation with Serum-Free Protein Block (Dako Cytomation) for 15 min and then incubation at 4°C overnight with primary antibody diluted in Dako antibody diluent. After several washes in PBS containing 0.1% BSA, 0.05% saponin, and 0.2% gelatin, sections were washed in PBS and incubated for 1 h with polymer-linked, peroxidase-conjugated goat anti-rabbit IgG (MACH2, Biocare Medical, Concord, CA), again washed with PBS, and then exposed to diaminobenzidine (DAB) for 5 min. Sections were washed in distilled water, dehydrated with xylene, mounted, and observed with light microscopy. Sections were examined on a Nikon E600 microscope equipped with CFI Plan Fluor ×40, numerical aperture 0.75 and CFI Plan Fluor ×10, numerical aperture 0.30 objectives using DIC optics and photographed using a DMX1200F digital camera and ACT-1 software (Nikon). Color correction was performed using Adobe Photoshop software (Adobe Systems, San Jose, CA).

Immunoblot analysis. Immunoblot analysis was performed as previously described (5, 6, 41–44, 46–48). Briefly, defined amounts, always identical in each lane of a gel, but typically 5–10 μg, of renal protein were electrophoresed on 10% PAGE ReadyGel (Bio-Rad, Hercules, CA). Gels were then transferred electrophoretically to nitrocellulose membranes, blocked with 5 g/dL nonfat dry milk in Blotto buffer (50 mM Tris, 150 mM NaCl, 5 mM Na_2EDTA, and 0.05% Tween 20, pH 7.6), and incubated at 4°C overnight with primary antibody diluted in nonfat dry milk. After being washed, membranes were exposed to secondary antibody, goat anti-rabbit IgG (Cell Signaling Technology, Beverly, MA) conjugated to horseradish peroxidase at a dilution of 1:5,000. Sites of antibody-antigen reaction were visualized using enhanced chemiluminescence (SuperSignal West Pico Substrate, Pierce) and a Kodak Image Station 440CF digital imaging system. Band density was normalized such that mean density in the same region (cortex or outer stripe of the outer medulla) in control tissues was 100.0. We confirmed the absence of saturation by examining pixel intensity distribution in all immunoblots.

In preliminary experiments, we found that a K^+-free diet had differing effects on expression of the putative "housekeeping proteins" β-actin and GAPDH, i.e., increasing expression of β-actin and decreasing expression of GAPDH. Accordingly, we were unable to normalize protein expression to housekeeping protein expression. In all experiments, we assessed loading and transfer equivalence using Ponceau S staining. Gels with evident differences between samples/lanes were discarded and not used for analysis.

Tissue section experiments of NCC phosphorylation. Mice were anesthetized with inhalant isoflurane anesthesia, and kidneys were perfused free of blood with CO_2- and HCO_3^--buffered solutions containing 8 mM K^+. Kidneys were removed rapidly, and 100-μm-thick transverse sections were cut on a vibrating microtome (Vi-

Table 1. *Antibodies used (alphabetical order)*

Antibody	Source	Dilutions Used
ENaCα	StressMarq Biosciences (SPC-403, Victoria, BC, Canada)	WB, 1:5,000
ENaCβ	StressMarq Biosciences (SPC-404, Victoria, BC, Canada)	WB, 1:5,000
ENaCγ	StressMarq Biosciences (SPC-405, Victoria, BC, Canada)	WB, 1:2,500
Glutamine synthetase	Abcam (ab73593, Cambridge, MA)	IHC, 1:10,000; WB, 1:1,500
H^+-ATPase, a4 subunit	Dr. Fiona Karet (Cambridge Institute for Medical Research, Cambridge, UK)	IHC, 1:50,000
Na^+-Cl^- cotransporter	Dr. David Ellison (Oregon Health Sciences University, Portland, OR)	IHC, 1:20,000; WB, 1:1,000
NBCe1-A	Michael F. Romero, Ph.D (α-333)	IHC, 1:2,000; WB, 1:1,000
Pan-NBCe1	ProteinTech	IHC, 1:1,000; WB, 1:2,000
Phosphate-dependent glutaminase	Dr. Norman Curthoys (Colorado State University)	WB, 1:3,000
Phospho*enol*pyruvate carboxykinase	Cayman Chemical Co. (no. 10004943, Ann Arbor, MI)	IHC, 1:5,000; WB, 1:2,000
Phospho-NCC	PhosphoSolutions (no. p1311-53, Aurora, CO)	IHC, 1:100,000; WB, 1:1,000
Rhbg	Generated in our laboratory	IHC, 1:20,000
Rhcg	Generated in our laboratory	IHC, 1:10,000

ENaC, epithelial Na^+ channel; NBCe1-A, Na^+-bicarbonate cotransporter electrogenic, isoform 1, splice variant A; Rh, Rhesus; WB, Western blot; IHC, immunohistochemistry.

bratome). Sections were then placed onto Transwell 24-mm-diameter filters, 0.4-μm pore size (Corning) into six-well plates with defined solutions containing varying amounts of K^+ and ammonia. Sections and solutions were then placed into a 5% CO_2 incubator maintained at 37°C and rocked gently to minimize unstirred layers. Tissues were removed from the incubator after completion of timed incubation, and protein extraction and immunoblot analysis for both phospho-NCC and total NCC were performed as detailed above. In preliminary experiments, similar results had been obtained with incubation for 1 and 2 h, and so the experiments reported were performed with a 1-h incubation.

We typically obtained 16–24 sections from a single kidney, enabling an average of 4 sections from a single kidney to be exposed to each experimental solution. We calculated the ratio of phospho-NCC to total-NCC, which we term the "NCC phosphorylation index" (NPI), in each section. This thereby controls for variations in the ratio of the cortex to renal medulla in each section. The NPI from all sections from a single kidney exposed to a particular medium composition was averaged to yield a single NPI that was used for statistical analysis. All tissue section NPI experiments used an equal number of male and female mouse kidneys. The sex of the kidney did not alter any of the responses observed.

All solutions contained (in mM) 106.9 NaCl, 2.0 NaH_2PO_4, 1.0 $MgSO_4$, 25 $NaHCO_3$, 8.33 glucose, 1.0 sodium acetate, and 1.2 $CaCl_2$. Solution K^+ and ammonia concentrations were altered by adding appropriate amounts of 1 mol/L KCl or NH_4Cl; osmolality was maintained constant by balanced addition of 1 mol/L choline-Cl. Solutions were bubbled with 95% O_2-5% CO_2 solutions for at least 20 min before use. Glutamine, alanine, and other amino acids were not included in the incubation medium so as to limit endogenous ammonia production. In preliminary experiments, this approach resulted in no detectable ammonia addition to the extracellular media by the sections.

NMR spectroscopy for 2-oxoglutarate quantification. Proton 1-D nuclear magnetic resonance (NMR) spectra were collected using a 14.1-T NMR magnet equipped with a CP TXI CryoProbe and an Avance II Console (Bruker Biospin, Billerca, MA). Each NMR sample consisted of 100 μL [50% (vol/vol), centrifuged and filtered] of urine, 80 μL [40% (vol/vol)] of deuterated 20× PBS, and 20 μL [10% (vol/vol)] of internal standard (5 mM DSS-D6 and 0.2% NaN_3 in D_2O, Chenomx, Alberta, Canada), making a total volume of 200 μL for a sample. The pH was controlled at 7.2. A 1-D NOESY pulse sequence (tnnoesy.c) was used to acquire 1-D proton spectra, with a 3-s relaxation delay (d1), 100-ms mixing time, 64 scans (nt), 12-ppm spectral width (sw), and 4 s of acquisition time (60). All experiments were acquired at 25°C. Spectra were processed and analyzed using MestReNova 11.0.0 (Mestrelab Research, Santiago de Compostela, Spain). They were zero filled to 131,072 points with exponential line broadening of 0.5 Hz and Whittaker Smoother baseline correction. Chemical shifts were calibrated with respect to DSS singlet signal at 0 ppm. 2-Oxoglutarate peaks were fitted to a mixed Gaussian-Lorentzian line shape and compared with the DSS standard to determine the concentration.

Real-time RT-PCR. We quantified H^+-K^+-ATPase (HK)α1 and HKα2 mRNA expression using Taqman-based real-time RT-PCR techniques, as previously described (20). Primer-probe sets for HKα1 and HKα2 were obtained from Applied Biosystems (HKα1: Mm00444423 and HKα2: Mm00446779). We used GAPDH as an internal control and quantified expression using the $2^{-\Delta C_T}$ method (where C_T is threshold cycle). Results were scaled such that mean expression in WT mice was 100.0.

Statistics. Results are presented as means ± SE; *n* refers to the number of animals studied. Statistical analysis was performed using ANOVA (general linear modeling). Specific subgroup differences were analyzed using a Student's *t* test with Bonferroni correction, as previously detailed (44, 45). When repeated measurements over time were obtained, statistical significance for the primary independent variable was determined using general linear model with repeated-measures analysis (IBM SPSS Statistics) followed by analysis at individual time points using Student's *t* test (44). In addition, we used Mauchly's test of sphericity when using repeated-measures ANOVA to evaluate whether the sphericity assumption was violated. All experiments included a similar number of male and female mice, and sex was included as a dependent variable in all statistical analyses; in no case did it change the statistical conclusions reached. *P* values of <0.05 were taken as statistically significant.

RESULTS

Effect of a K^+-free diet on WT and NBCe1-A KO mice. Exposure to a K^+-free diet, compared with a K^+-control diet, induced a number of physiological changes. Table 2 shows these responses. Body weight was lower in NBCe1-A KO mice on both diets, similar to previously reported results while on normal diet (45). Daily food intake when adjusted for body weight did not differ significantly. Serum K^+ was lower in NBCe1-A KO mice on both diets, and serum K^+ decreased significantly in response to K^+-free diet in both genotypes.

Table 2. *Physiological parameters in NBCe1-A KO mice*

Parameter	WT	NBCe1-A KO	*P* Value
Physiological parameters on K^+-control diet			
Mean body weight, g	23.5 ± 1.2 (16)	18.1 ± 0.8 (16)	<0.001
Mean daily food intake, g/day	4.3 ± 0.1 (16)	3.9 ± 0.2 (16)	<0.05
Mean daily food intake, g/g body wt	0.19 ± 0.01 (16)	0.22 ± 0.01 (16)	NS
Urine pH	6.50 ± 0.11 (16)	5.37 ± 0.11 (16)	<0.001
Urine ammonia, μmol/day	123 ± 26 (16)	157 ± 24 (16)	NS
Serum Na^+, mM	152 ± 1 (9)	150 ± 1 (9)	<0.05
Serum K^+, mM	4.49 ± 0.14 (9)	3.73 ± 0.13 (9)	<0.05
Serum HCO_3^-, mM	21.5 ± 1.3 (9)	12.4 ± 0.5 (9)	<0.001
Physiological parameters on K^+-free diet			
Mean body weight, g	26.2 ± 1.1 (11)	18.3 ± 0.7 (11)	<0.001
Mean daily food intake, g/day	5.4 ± 0.1 (11)	3.7 ± 0.1 (11)	<0.001
Mean daily food intake, g/g body wt	0.21 ± 0.01 (11)	0.21 ± 0.01 (11)	NS
Serum Na^+, mM	152 ± 2 (11)	149 ± 1 (11)	NS
Serum K^+, mM	3.50 ± 0.18 (11)	2.50 ± 0.16 (11)	<0.001
Serum HCO_3^-, mM	23.8 ± 0.9 (11)	11.8 ± 0.6 (11)	<0.001

Values are means ± SE. Numbers in parentheses are numbers of animals in each group. NBCe1-A KO, Na^+-bicarbonate cotransporter electrogenic, isoform 1, splice variant A knockout; WT, wild type; NS, not significant.

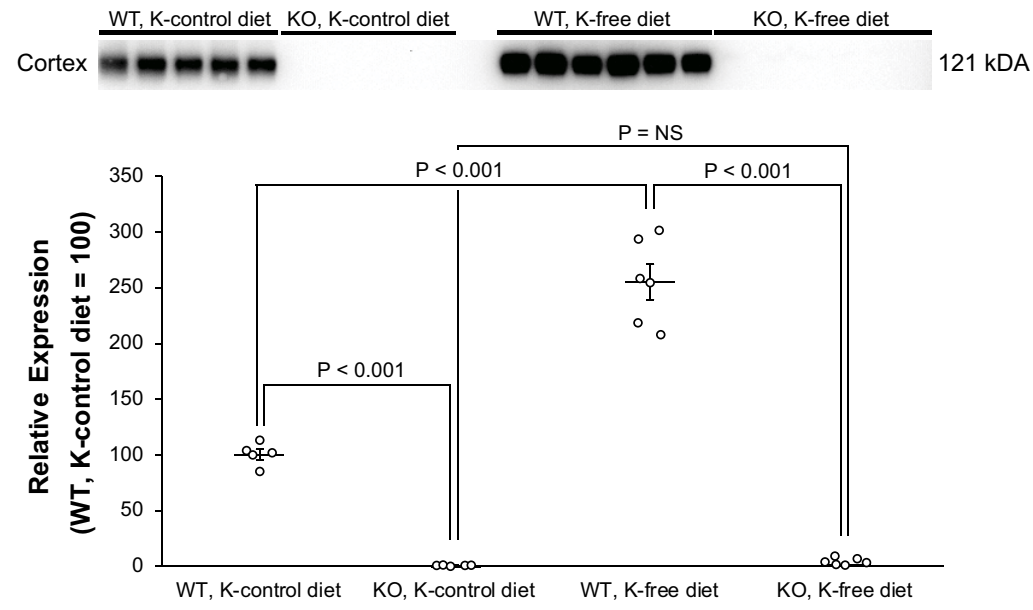

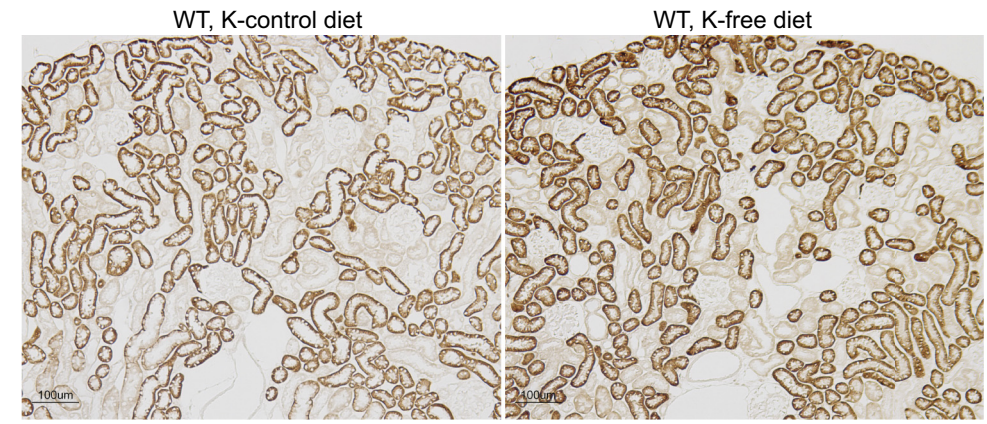

Fig. 1. Effect of K^+-free diet on Na^+-bicarbonate cotransporter electrogenic, isoform 1, splice variant A (NBCe1-A) expression. *A*: effect of K^+-free diet on NBCe1-A expression in wild-type (WT) mice. *Top*: WT mice provided K^+-free diet for 4 days exhibited significantly greater NBCe1-A expression than did mice provided K^+ control diet. *B*: NBCe1-A immunolabel in cortex of WT mice provided either K^+ control diet or K^+-free diet. NBCe1-A immunolabel intensity in cortical proximal tubule segments was greater in WT mice on K^+-free diet than in those on K^+ control diet. NBCe1-A immunolabel was not detectable in the outer stripe of the outer medulla (OSOM) in either condition (data not shown). Immunolabel results are representative of findings in 5 mice on K^+ control diet and 6 mice on K^+-free diet.

Serum bicarbonate[2] in WT mice averaged 21.5 ± 1.3 mM on K^+ control diet and 23.8 ± 0.9 mM after 4 days of K^+-free diet (n = 9 and 11, respectively). In KO mice, baseline serum bicarbonate concentration was lower than in WT on K^+-control diet, 12.4 ± 0.5 mM, similar to our previous report (45), and averaged 11.8 ± 0.6 mM after 4 days of K^+-free diet (n = 9 and 11, respectively). NBCe1-A deletion tended to alter the serum bicarbonate response to K^+-free diet, but this effect did not meet statistical significance ($P < 0.08$ by ANOVA).

Effect of K^+-free diet on NBCe1-A expression. Hypokalemia increases both proximal tubule bicarbonate reabsorption (9, 11) and ammonia generation (34, 51, 54). We first examined whether exposure to a K^+-free diet is associated with increased NBCe1-A expression. Immunoblot analysis of tissues from mice exposed to a K^+-free diet for 4 days using a NBCe1-A-specific antibody showed a significant increase in NBCe1-A expression (Fig. 1*A*). There was no detectable NBCe1-A protein expression in NBCe1-A KO mice either on a K^+-control diet or K^+-free diet, confirming the specificity of this antibody. Immunohistochemistry (Fig. 1*B*) showed increased basolateral NBCe1-A immunolabel intensity in cortical proximal tubule segments. In proximal tubule segments in the outer stripe of the outer medulla, there was no detectable NBCe1-A immunolabel either in WT or KO kidneys. Thus, diet-induced hypokalemia increases cortical proximal tubule NBCe1-A expression.

The proximal tubule expresses a second splice variant of the NBCe1 gene, NBCe1-B (20). We used an antibody that recognizes NBCe1-B in the NBCe1-A KO kidney to examine the NBCe1-B response to a K^+-free diet (20). In the cortex of NBCe1-A KO mice, NBCe1-B protein expression did not change significantly in response to the K^+-free diet, but its

[2] Both serum HCO_3^- and P_{CO_2} determine arterial pH. P_{CO_2} is determined by minute ventilation, a pulmonary response, and not by renal acid-base mechanisms. We believe it is possible that the anesthesia and laparotomy required for blood collection can alter minute ventilation and, if so, would rapidly change arterial blood P_{CO_2} and pH. We were unable to measure minute ventilation in our anesthetized mice and therefore cannot confirm that measured P_{CO_2} and pH accurately reflect P_{CO_2} and pH in nonanesthetized, nonrestrained mice. Because of these considerations, although we measured these values we do not report them.

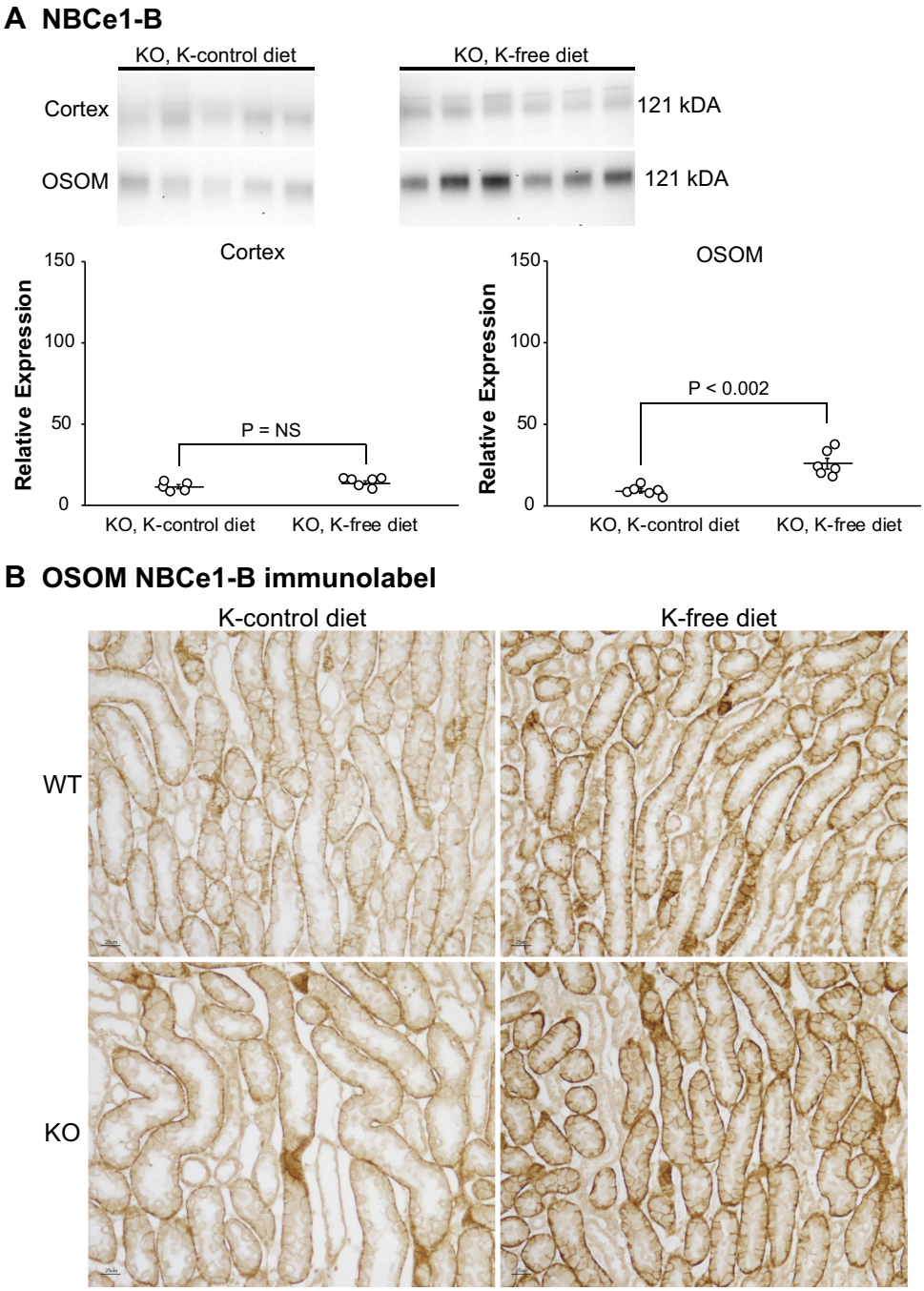

Fig. 2. Effect of K^+-free diet on Na^+-bicarbonate cotransporter electrogenic, isoform 1, splice variant B (NBCe1-B) expression. *A*: NBCe1-B expression response in NBCe1-A knockout (KO) mice. Because the mouse kidney expresses both NBCe1-A and NBCe1-B, and only NBCe1-B in the NBCe1-A KO mouse (20), the pan-NBCe1 antibody used, which recognizes all NBCe1 splice variants, is specific in the kidney for NBCe1-B. NBCe1-B expression did not differ in the cortex between mice provided K^+ control diet and those provided K^+-free diet. In the outer stripe of the outer medulla (OSOM), mice provided K^+-free diet had significantly greater NBCe1-B expression than mice provided K^+ control diet. *B*: NBCe1-B immunolabel in the OSOM, where NBCe1-B is the only expressed NBCe1 variant (20). In both wild-type (WT) and KO mice, proximal straight tubule basolateral NBCe1-B immunolabel was more intense in mice provided K^+-free diet than in those provided K^+ control diet; $n = 5$ mice on K^+ control diet and 6 mice on K^+-free diet for NBCe1-B in both immunoblot analysis and immunolabel results.

expression in the outer medulla increased significantly (Fig. 2*A*). In both WT and KO mice, immunohistochemistry showed increased proximal tubule basolateral NBCe1 immunolabel intensity in the outer stripe of the outer medulla in response to diet-induced hypokalemia (Fig. 2*B*). Since NBCe1-A is not expressed in this portion of the proximal tubule, and NBCe1-B is the only other NBCe1 splice variant present in the mouse kidney (20), these results indicated that diet-induced hypokalemia also increases NBCe1-B expression in the proximal straight tubule in the outer medulla.

Effect of NBCe1-A deletion on the ammonia response to hypokalemia. We then determined the effect of NBCe1-A deletion on the urinary ammonia response to hypokalemia. Table 2 shows key physiological parameters in these mice. While mice were on the K^+ control diet, urine ammonia excretion did not differ significantly between WT and NBCe1-A KO mice (Fig. 3*A*). When they were transitioned to the K^+-free diet, urine ammonia excretion increased in WT mice on the first day and remained elevated throughout the entire experimental period. The response of NBCe1-A KO mice to the K^+-free diet was blunted significantly ($P < 0.01$ by ANOVA). On each day of the K^+-free diet, the increase in ammonia excretion above baseline was significantly less than in WT mice, and on *days 3* and *4*, urinary ammonia excretion did not differ significantly from control diet rates (Fig. 3*B*). Quantitatively, NBCe1-A deletion decreased the ammonia ex-

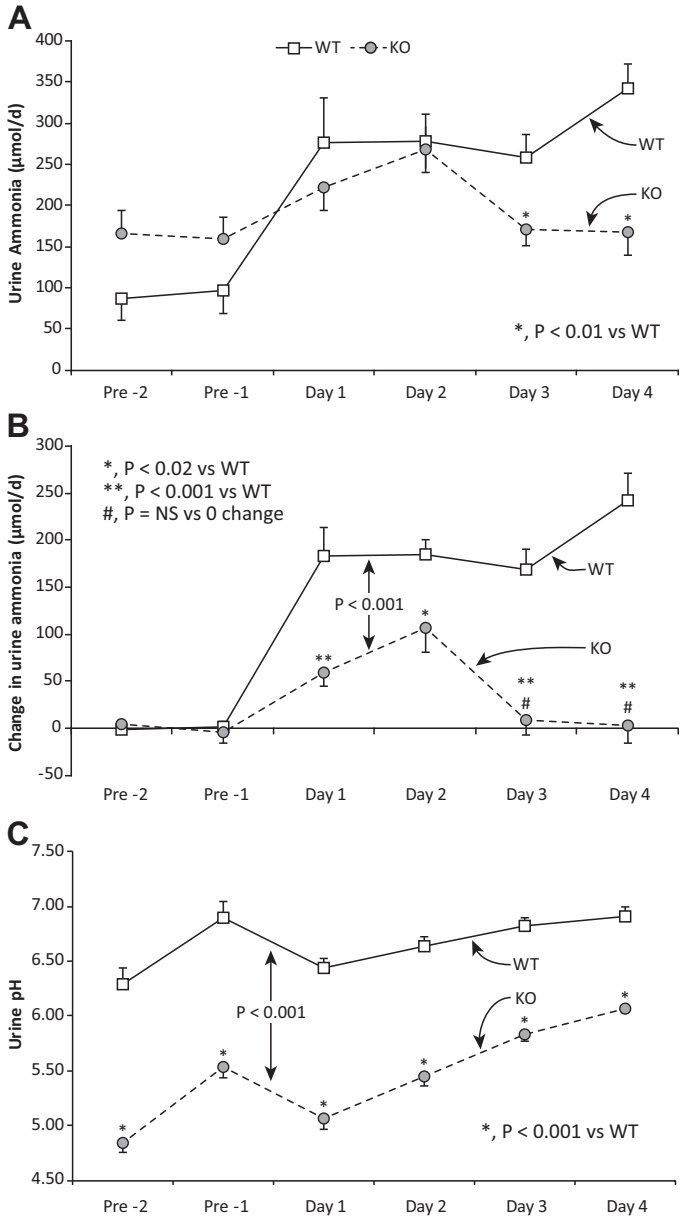

Fig. 3. Na^+-bicarbonate cotransporter electrogenic, isoform 1, splice variant A (NBCe1-A) deletion blocks the urinary ammonia response to hypokalemia. *A*: urinary ammonia excretion in wild-type (WT) and NBCe1-A knockout (KO) mice. Ammonia excretion on K^+ control diet (Pre-2 and Pre-1 days) tended to be higher in KO mice but did not differ significantly. "Pre-2" and "Pre-1" refer to the 2 days on K^+ control diet before the K^+-free diet. Urine ammonia was significantly less in KO than in WT mice on *days 3* and *4* of K^+-free diet. *B*: change in ammonia excretion from baseline (mean of Pre-2 and Pre-1) in response to K^+-free diet. WT mice had a rapid increase in ammonia excretion, whereas KO mice had a transient and significantly suppressed increase on *days 1* and *2* and then no significant change from baseline on *days 3* and *4* of K^+-free diet. *C*: urine pH response. Urine pH was significantly lower under basal conditions in KO mice than in WT mice and remained significantly lower during each day of K^+-free diet. Thus, the decreased ability to excrete ammonia cannot be ascribed to defective urine acidification in KO mice. Error bars are not shown when they are smaller than the symbol for mean value; $n = 17$ for each genotype.

cretion change by 78 ± 6% ($n = 11$ in each group, $P < 0.001$). Analysis of body weight-adjusted changes in urinary ammonia did not change these conclusions. Thus, NBCe1-A is essential to the urinary ammonia response to hypokalemia.

The ability to acidify urine is critical for ammonia excretion. NBCe1-A KO mice excreted a more acidic urine than did WT mice under both K^+-control and K^+-free dietary conditions (Fig. 3*C*). Thus, the absence of an increase in ammonia excretion in NBCe1-A KO mice is not due to an impaired ability to acidify the urine.

Proximal tubule ammonia generation of enzymes. Urinary ammonia, in contrast to most other urinary solutes, derives predominantly from intrarenal generation, predominantly in the proximal tubule, and not from arterial delivery. The first enzyme involved in ammoniagenesis is mitochondrial phosphate-dependent glutaminase (PDG). In the cortex, where NBCe1-A is present in WT mice, NBCe1-A deletion blunted the increase induced by a K^+-free diet ($P < 0.05$ by ANOVA; Fig. 4*A*). This effect was limited to the cortex; NBCe1-A deletion did not alter either basal or the hypokalemia-induced increase in PDG expression in the outer medulla [P = not significant (NS) by ANOVA].

A key cytoplasmic enzyme involved in ammonia generation is phospho*enol*pyruvate carboxykinase (PEPCK). NBCe1-A deletion decreased cortical PEPCK expression significantly in mice fed the K^+-control diet, and it decreased the response to the K^+-free diet ($P < 0.001$ by ANOVA; Fig. 4*B*). Thus, in cortical proximal tubule segments, NBCe1-A is necessary for the PEPCK response to hypokalemia. In contrast, in the outer medulla, where NBCe1-A is not present, PEPCK was significantly greater in NBCe1-A KO mice compared with WT mice, both on K^+ control and K^+-free diets, and the increase in PEPCK induced by the K^+-free diet was greater in NBCe1-A KO mice ($P < 0.001$ by ANOVA).

PEPCK immunohistochemistry showed similar findings. While on the K^+-control diet, PEPCK immunolabel intensity was substantially less in KO mice than in WT mice in the proximal convoluted tubule (PCT) and proximal straight tubule in the medullary ray (PST-MR) (Fig. 4*C*). Immunolabel intensity increased in response to the K^+-free diet in WT mice. In KO mice, the K^+-free diet-induced increase in cortical proximal tubule PEPCK immunolabel intensity was substantially less than in WT mice. In the proximal straight tubule in the outer medulla (PST-OM), immunolabel intensity was slightly greater in KO mice than in WT mice while on the K^+-control diet. The K^+-free diet increased immunolabel intensity in the PST-OM of WT and KO mice, and the increase was greater in KO mice.

Proximal tubule ammonia recycling enzyme glutamine synthetase response. A third key component of ammonia generation involves ammonia recycling via the enzyme glutamine synthetase (GS). Conditions that increase ammonia excretion, such as metabolic acidosis and hypokalemia, decrease GS expression (15, 43, 76, 86). The K^+-free diet decreased cortical GS expression in both genotypes, but the suppression was blocked significantly by NBCe1-A KO ($P < 0.01$ by ANOVA; Fig. 5*A*). In the outer medulla, where NBCe1-A is not normally expressed, the K^+-free diet-induced decrease in GS expression was accentuated by NBCe1-A deletion ($P < 0.001$ by ANOVA).

Immunohistochemistry examining GS immunolabel showed similar findings (Fig. 5*B*). In cortical proximal tubule segments, PCT and PST-MR, GS immunolabel intensity did not differ between WT and KO mice on the K^+-control diet. In mice exposed to the K^+-free diet, PCT and PST-MR GS

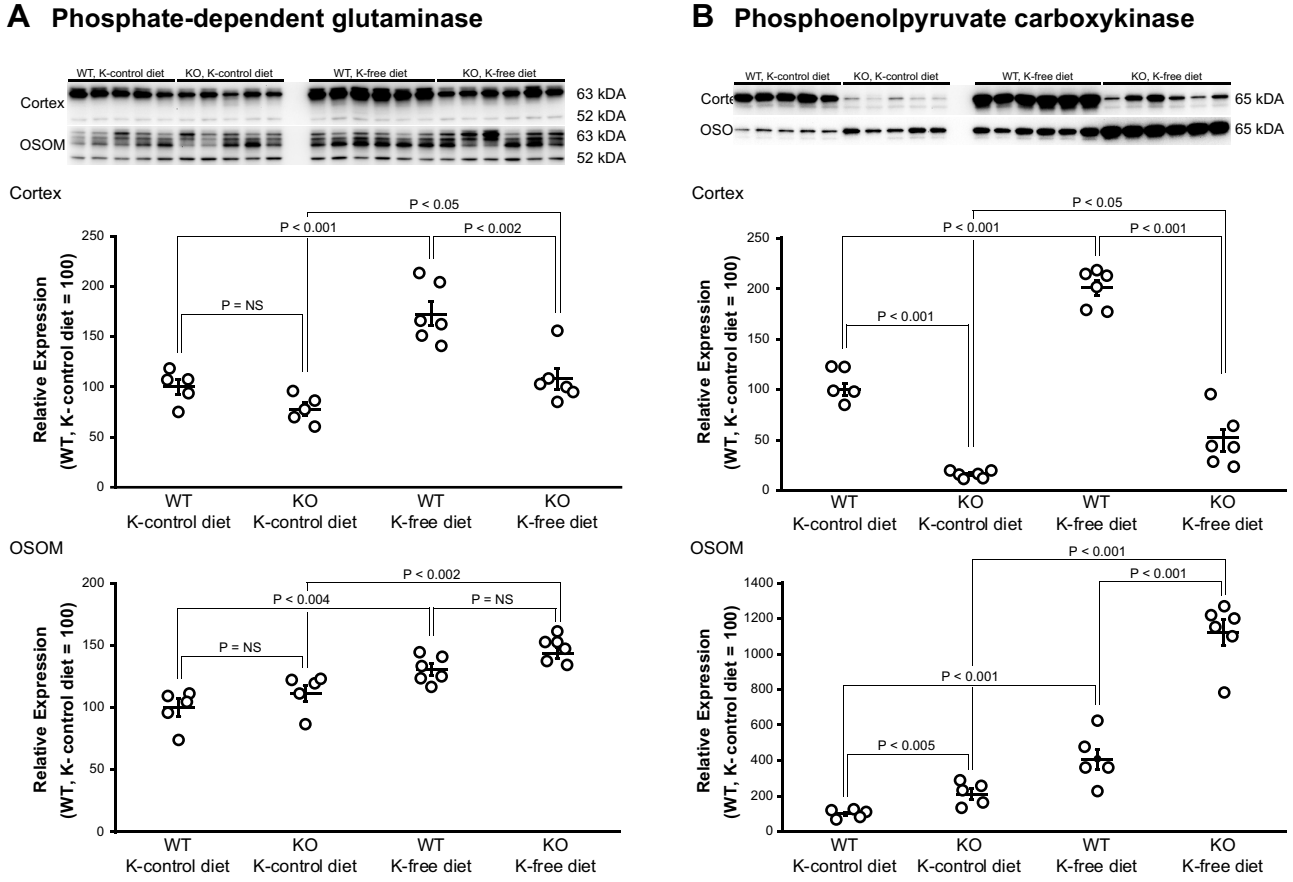

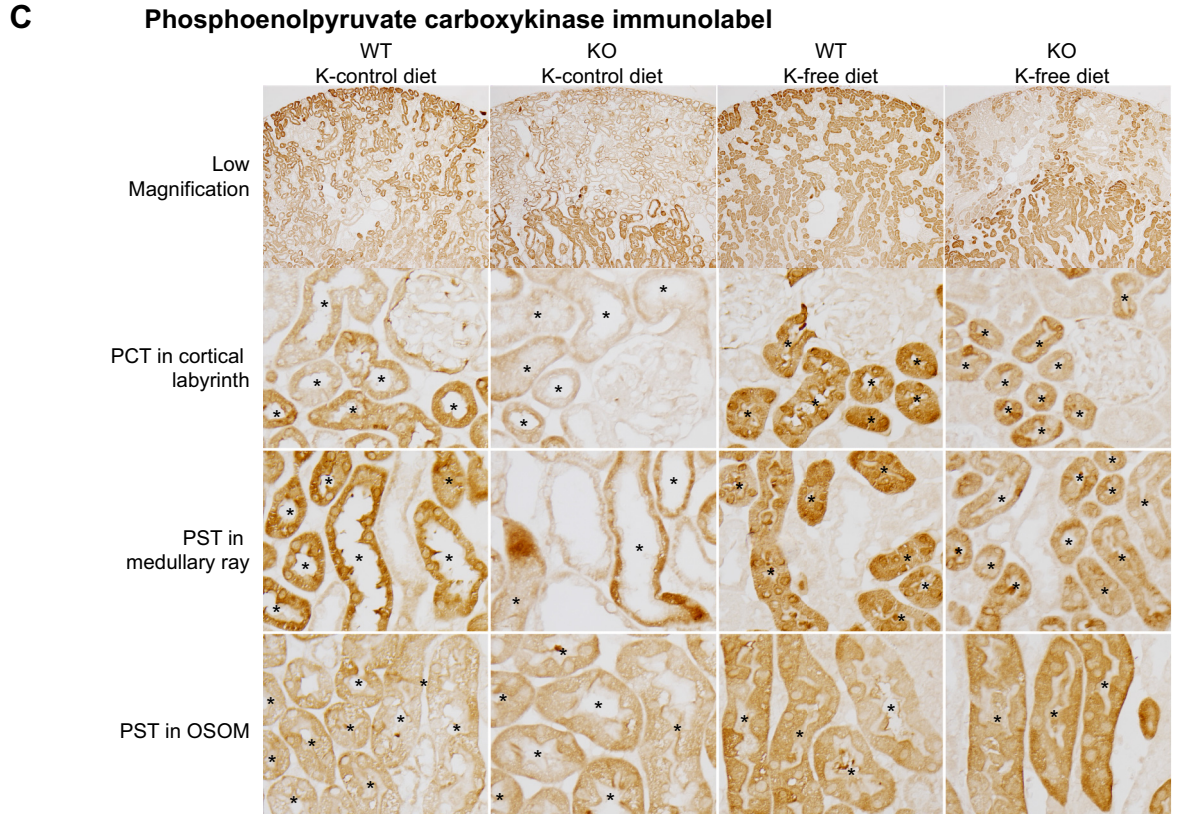

immunolabel intensity decreased in both genotypes, but the decrease was less in KO mice (Fig. 4). In the PST-OM, GS immunolabel intensity was similar in WT and KO mice on the K^+-control diet, consistent with the minimal, ~10%, difference by immunoblot analysis. In hypokalemic WT and KO mice, immunolabel intensity decreased in the PST-OM, and the magnitude of decrease was greater in KO mice, consistent with immunoblot results.

Thus, in cortical proximal tubule segments that normally express NBCe1-A, its deletion blunts the expected change in response to hypokalemia in enzymes involved in both ammonia generation (PDG and PEPCK) and ammonia recycling (GS). In the outer medulla, the responses of both PEPCK and GS are accentuated, suggesting adaptive responses in PST-OM to the NBCe1-A deletion in cortical proximal tubule segments.

Ammonia transport proteins. Ammonia produced in the kidney undergoes regulated transport across epithelial cells via specific transport proteins. H^+-ATPase is critical for collecting duct ammonia secretion through its role in H^+ secretion (7, 78, 83, 84). Immunohistochemistry comparing WT and KO mice on the K^+-free diet showed no evident difference in H^+-ATPase expression or membrane polarization (Fig. 6*A*). Rh glycoproteins have a critical role in collecting duct ammonia secretion (53, 81, 83, 85). Immunohistochemistry comparing WT and KO mice on the K^+-free diet also showed no detectable difference in either Rhbg or Rhcg expression (Figs. 6, *B* and *C*, respectively). Thus, the failure of increased ammonia excretion in response to hypokalemia in NBCe1-A KO mice is unlikely to have been the result of abnormal expression of these proteins.

Effect of NBCe1-A deletion on K^+ homeostasis. Serum electrolyte analysis showed a surprising effect of NBCe1-A deletion on K^+ homeostasis. Serum K^+ on control diet was significantly less in KO mice than in WT mice (WT: 4.49 ± 0.14 mM and KO: 3.73 ± 0.13 mM, $n = 9$ in each group, $P < 0.002$). After 4 days of the K^+-free diet, serum K^+ decreased in each group and remained significantly lower in NBCe1-A KO mice (WT: 3.50 ± 0.18 mM and KO: 2.50 ± 0.16 mM, $n = 11$ in each group, $P < 0.001$). Thus, NBCe1-A deletion resulted in significantly lower serum K^+, both on the K^+ control diet and after 4 days of the K^+-free diet. Figure 7*A* shows these findings.

Effect on K^+ excretion. The primary K^+ homeostatic response to a K^+-free diet involves a rapid decrease in urinary K^+ excretion. While on the K^+ control diet, K^+ excretion did not differ significantly between WT and KO mice (WT: 813 ± 57 μmol/day and KO: 670 ± 44 μmol/day, $n = 17$ mice/genotype, P = NS). Changing to K^+-free diet decreased K^+ excretion in both genotypes, but NBCe1-A KO mice excreted significantly more urinary K^+ than did WT mice on each day of the K^+-free diet (Fig. 7*B*). Mean daily K^+ excretion over the 4 days was ~50% greater in KO mice than in WT mice (WT: 58 ± 5 μmol/day and KO: 88 ± 14 μmol/day, $n = 17$ mice/genotype, $P < 0.001$). Thus, NBCe1-A deletion, despite resulting in more severe hypokalemia, resulted in less ability to conserve K^+ in response to a K^+-free diet.

Phosphorylated NCC response to K^+-free diet. The distal convoluted tubule (DCT) NCC has a key role in K^+ homeostasis. NCC phosphorylation induces its translocation to the apical plasma membrane, where it is functionally active (90). This increases DCT NaCl reabsorption and decreases Na^+ delivery to the collecting duct, where Na^+ reabsorption is coupled to K^+ secretion (4, 10, 27, 62, 77). Phosphorylated (p-)NCC expression increased in both genotypes in response to K^+-free diet, but the increase was significantly less in NBCe1-A KO mice ($P < 0.05$ by ANOVA; Fig. 8*A*). Total NCC was significantly increased by both NBCe1-A deletion and by K^+-free diet ($P < 0.05$ and $P < 0.001$, respectively, by ANOVA), but genotype did not alter the response to K^+-free diet (P = NS by ANOVA). The ratio of p-NCC to total NCC did not differ between WT and KO mice on the K^+ control diet, and it increased in both genotypes in response to K^+-free diet, but the increase was significantly less in NBCe1-A KO mice ($P < 0.001$ by ANOVA; Fig. 8*C*). p-NCC immunolabel intensity showed similar findings (Fig. 8*D*).

We also examined the correlation between plasma K^+ and p-NCC, total NCC, and the p-NCC-to-total NCC ratio. Figure 9 shows this correlation. ANOVA showed a significant correlation of both p-NCC and the p-NCC-to-total NCC ratio with plasma K^+ ($P < 0.001$ by ANOVA for each). In addition, there was also a significant and independent effect of NBCe1-A deletion on both p-NCC and the p-NCC-to-total NCC ratio ($P < 0.001$ for each). Total NCC expression also correlated significantly with plasma K^+ ($P < 0.005$ by ANOVA), but NBCe1-A deletion did not have an independent association (P = NS by ANOVA).

NCC phosphorylation on normal chow. The finding that NBCe1-A KO mice on the K^+ control diet had mildly lower serum K^+ than did WT mice without a parallel increase in p-NCC expression may be related to unidentified effects of the K^+ control diet. We (45) have previously reported that serum

Fig. 4. Na^+-bicarbonate cotransporter electrogenic, isoform 1, splice variant A (NBCe1-A) deletion blunts the response of cortical proximal tubule ammoniagenic enzymes to hypokalemia. *A*: effects of NBCe1-A deletion on phosphate-dependent glutaminase (PDG) expression response to K^+-free diet. While on K^+ control diet, PDG expression did not differ significantly between wild-type (WT) and NBCe1-A knockout (KO) mice in either the cortex or outer stripe of outer medulla (OSOM). Exposure to K^+-free diet for 4 days increased PDG expression significantly in both the cortex and OSOM. In the cortex, the magnitude of increase was significantly less in KO mice than in WT mice, whereas the increase did not differ in the OSOM. *B*: phospho*enol*pyruvate carboxykinase (PEPCK) response. In the cortex, NBCe1-A KO decreases PEPCK expression significantly, both on K^+ control diet and after exposure to K^+-free diet, and both genotypes increased significantly in response to K^+-free diet. In the OSOM, where NBCe1-A is not expressed, KO mice had significantly greater PEPCK expression under basal conditions than did WT mice. Exposure to K^+-free diet increased PEPCK expression in the OSOM in both genotypes, but the increase was significantly greater in KO mice than in WT mice. *C*: effects of NBCe1-A deletion and K^+-free diet on PEPCK immunolabel. KO mice had less intense PEPCK immunolabel in proximal convoluted tubule (PCT) segments in the cortical labyrinth than did WT mice while on K^+-control diet. After exposure to K^+-free diet for 4 days, PEPCK immunolabel intensity increased in both genotypes but remained substantially less in KO mice than in WT mice. Cortical proximal straight tubule (PST) segments in the medullary ray exhibited a similar pattern of PEPCK immunolabel intensity. In PST segments in the OSOM, PEPCK intensity was greater in KO mice than in WT mice while on K^+ control diet. After exposure to K^+-free diet, PEPCK immunolabel intensity increased in OSOM PST in both genotypes but remained substantially greater in KO mice than in WT mice. *Proximal tubule lumen. Immunoblot analysis and micrographs are representative of findings in 5 mice on K^+ control diet and 6 on K^+-free diet in each genotype.

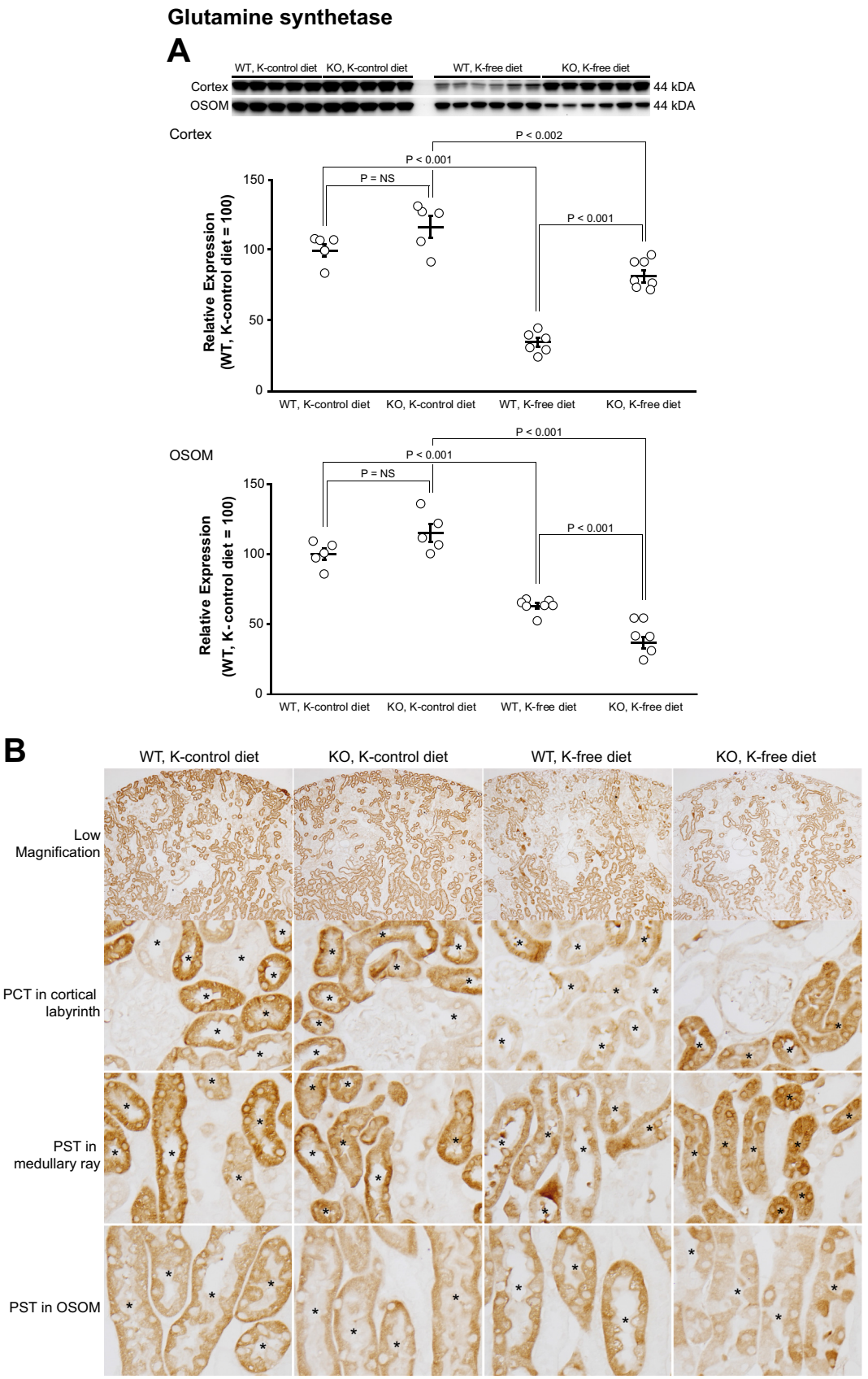

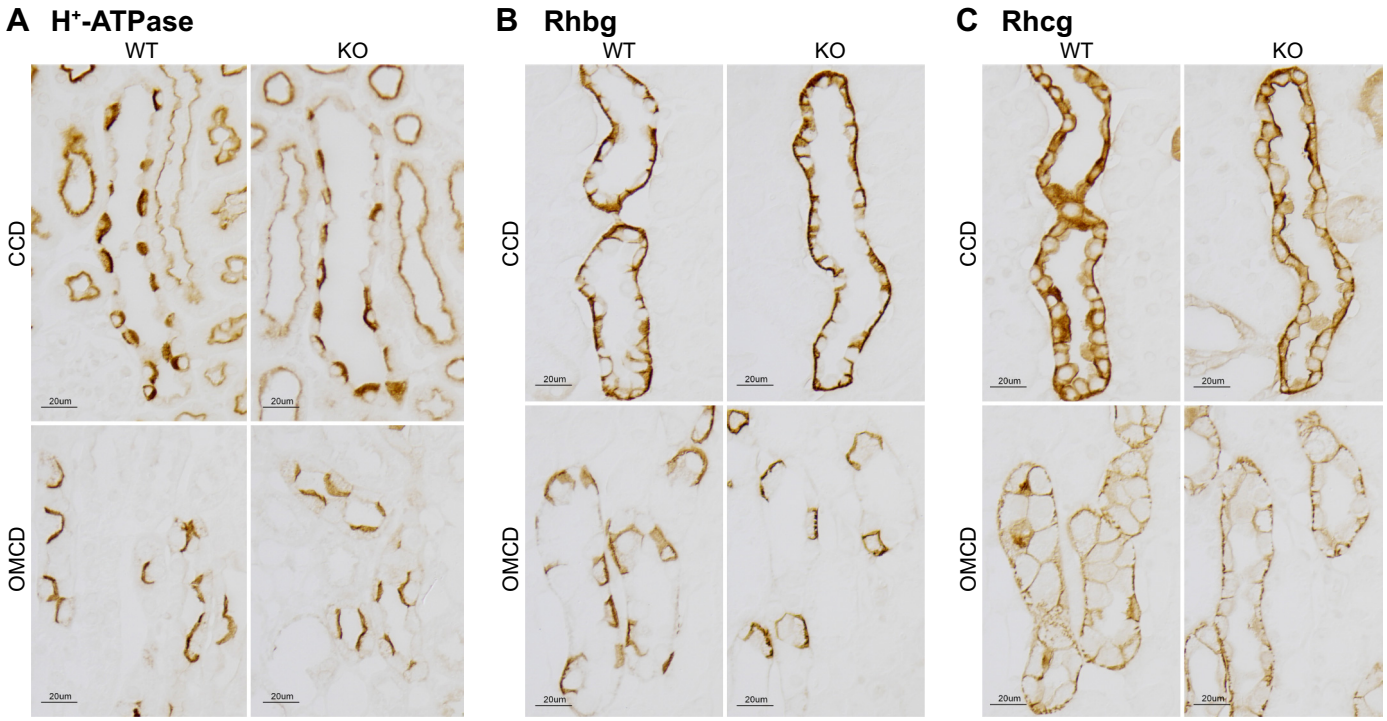

Fig. 6. Effect of Na^+-bicarbonate cotransporter electrogenic, isoform 1, splice variant A (NBCe1-A) deletion on collecting duct H^+-ATPase and Rhesus (Rh) glycoprotein expression in mice on K^+-free diet. *A*: H^+-ATPase immunolabel in the cortical collecting duct (CCD) and outer medullary collecting duct (OMCD). There was no detectable difference in H^+-ATPase immunolabel between hypokalemic wild-type (WT) and NBCe1-A knockout (KO) mice in either the CCD or OMCD. *B*: Rhbg immunolabel. There was no detectable difference in Rhbg immunolabel between hypokalemic WT and KO mice in either the CCD or OMCD. *C*: Rhcg immunolabel. There was no detectable difference in Rhcg immunolabel between hypokalemic WT and KO mice in either the CCD or OMCD. Results are representative of findings from 6 mice in each genotype.

K^+ does not differ significantly between WT and NBCe1-A KO mice when fed standard rodent chow. Both p-NCC and total NCC expression in mice on normal rodent chow, examined in a subset of tissues from previous studies, were greater in KO mice than in WT mice (Fig. 10, *A* and *B*). The p-NCC-to-total NCC ratio did not differ significantly between WT and KO mice (Fig. 10*C*). This suggests that, while on normal rodent chow, NBCe1-A KO mice maintain normal serum K^+ by increasing p-NCC and total NCC expressions but that this does not occur while on a K^+ control diet.

Effect of ammonia on NCC phosphorylation. Our finding that both ammonia metabolism and NCC phosphorylation responses to the K^+-free diet were impaired in NBCe1-A KO mice suggests the possibility that ammonia alters the NCC phosphorylation response. To examine this, we determined the effect of extracellular ammonia on NCC phosphorylation in freshly isolated kidney sections from WT C57BL/6 mice. Because of the possibility of a differing ratio of the cortex versus medulla in different sections, which would alter the relative number of NCC-expressing DCT cells, all comparisons involved assessment of the p-NCC-to-total NCC ratio in each section. We use the term NPI to refer to the ratio of p-NCC to total NCC. As shown in Fig. 11*A*, changing extracellular K^+ exerted the expected increase in NPI. Inclusion of ammonium chloride in the extracellular media significantly inhibited, albeit only to a small extent, NPI in sections exposed to 2 mM K^+ (Fig. 11*B*). In sections exposed to 6 mM K^+, ammonia slightly increased NPI. Finally, we determined the effect of ammonia on NPI across of range of potassium concentrations from 2 to 8 mM (Fig. 11*C*). Figure 11*D* shows the effect of ammonia on NCC phosphorylation at each K^+ concentration (results are log transformed so that inhibition and stimulation have similar magnitude changes in the figure). Ammonia addition decreased NCC phosphorylation at both 2 and 4 mM K^+ and increased it at 6 and 8 mM. Thus, the effect of NBCe1-A deletion to inhibit NCC phosphorylation in response to diet-induced hypokalemia cannot be attributed to the inhibition of ammonia metabolism.

Fig. 5. Na^+-bicarbonate cotransporter electrogenic, isoform 1, splice variant A (NBCe1-A) deletion blocks the response of cortical proximal tubule ammonia recycling enzyme glutamine synthetase (GS) to hypokalemia. *A*: effect of NBCe1-A deletion on GS expression in response to hypokalemia by immunoblot analyses. GS expression in the cortex and in outer stripe of the outer medulla (OSOM) did not differ significantly between wild-type (WT) and NBCe1-A knockout (KO) mice on K^+ control diet. Exposure to K^+-free diet decreased GS expression in both genotypes in both the cortex and OSOM. The decrease was blunted significantly in the cortex in KO mice. In contrast, in the OSOM, the decrease was accentuated significantly. *B*: effects of NBCe1-A KO and K^+-free diet on GS immunolabel intensity. While on K^+ control diet, GS immunolabel intensity in proximal convoluted tubule (PCT) segments in the cortical labyrinth, in the medullary ray, and in the OSOM did not differ significantly between WT and KO mice. Exposure to K^+-free diet decreased immunolabel intensity in cortical proximal tubule segments (PCT and PST in medullary ray), but the magnitude of the decrease was greater in WT mice than in KO mice. In PST in the OSOM, in contrast, immunolabel intensity was less in KO mice than in WT mice. *Proximal tubule lumen. Immunolabel micrographs are representative of findings in 5 mice on K^+ control diet and 6 mice on K^+-free diet in each genotype.

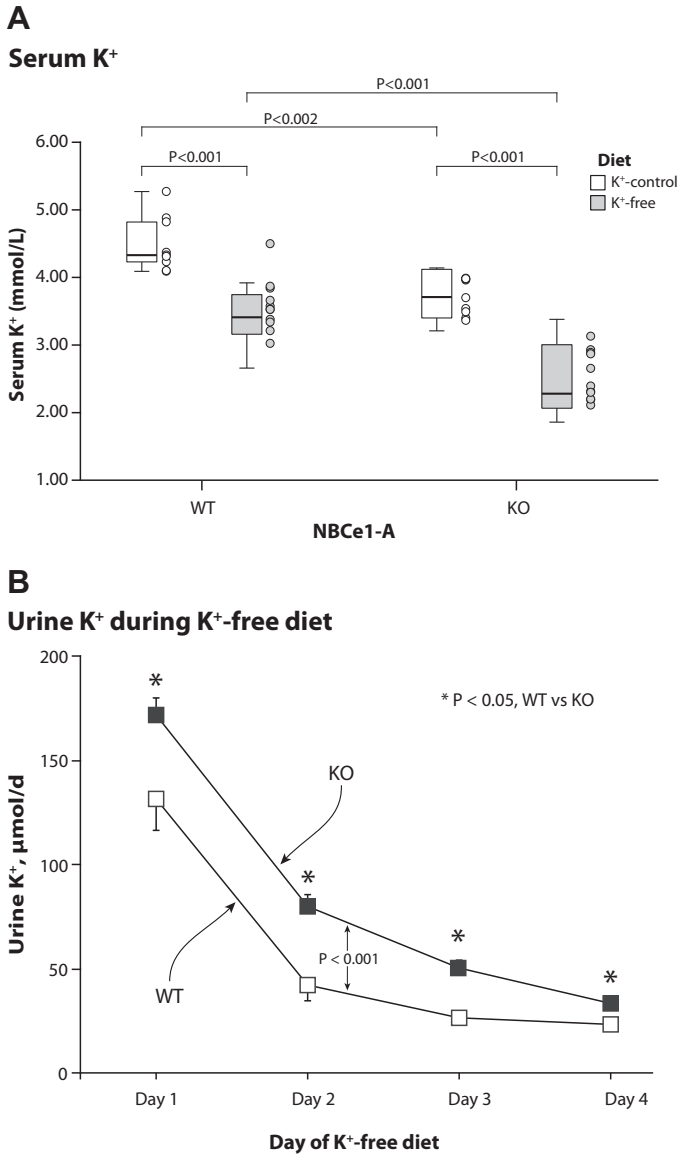

Fig. 7. Na^+-bicarbonate cotransporter electrogenic, isoform 1, splice variant A (NBCe1-A) deletion alters K^+ homeostasis. *A*: serum K^+ in wild-type (WT) and NBCe1-A knockout (KO) mice on either K^+ control diet or K^+-free diet. Serum K^+ was lower in NBCe1-A KO mice than in WT mice both while on K^+ control diet and after 4 days of K^+-free diet. *B*: urinary K^+ excretion on each day of K^+-free diet. Urinary K^+ was significantly greater in NBCe1-A KO mice than in WT mice on each day of K^+-free diet. Not shown is that urinary K^+ did not differ between WT and KO mice while on K^+ control diet; $n = 17$ in each genotype for urinary K^+ measurements. $^*P < 0.05$ vs. WT mice on a specific day.

Effect of metabolic acidosis on NCC phosphorylation. We next considered the possibility that the impaired NCC phosphorylation in hypokalemic NBCe1-A KO mice in the present study was related to the systemic acidosis present in NBCe1-A KO mice. To do so, we examined NCC phosphorylation in tissues obtained in our recent report examining the effect of acid loading on WT and NBCe1-A KO mice (45). As shown in Fig. 10, in vivo acid loading did not alter significantly either absolute p-NCC expression (Fig. 10*A*), total NCC (Fig. 10*B*), or the p-NCC-to-total NCC ratio in either KO or WT mice (Fig. 10*C*).

We also examined the effect of ex vivo metabolic acidosis on NCC phosphorylation. Using tissue sections, we determined whether a bicarbonate concentration of 12 mM, compared with 25 mM, altered NPI at either 2 or 6 mM K^+. Our results showed that NPI was unaffected by this change in extracellular bicarbonate (Fig. 12). These findings suggest that metabolic acidosis does not explain the impaired NCC phosphorylation response of NBCe1-A KO mice to a K^+-free diet.

Effect of NBCe1-A deletion on 2-oxoglutarate. The organic anion 2-oxoglutarate has intrarenal cell signaling effects (26, 57). Single cell mRNA sequencing showed expression of its canonical receptor, *Oxgr1*, in DCT cells, A- and B-type intercalated cells, and non-A, non-B intercalated cells (59). Because the proximal tubule is the primary site determining 2-oxoglutarate excretion, we evaluated whether NBCe1-A deletion alters urinary 2-oxoglutarate. On the K^+ control diet, urinary 2-oxoglutarate did not differ significantly between WT and KO mice (Table 3). Feeding the same mice a K^+-free diet for 4 days decreased urinary 2-oxoglutarate significantly in both genotypes, and the final urinary 2-oxoglutarate excretion did not differ significantly between WT and KO mice (P = NS). This indicates that differences in proximal tubule 2-oxoglutarate metabolism are unlikely to mediate the observed changes in either NCC phosphorylation or distal nephron K^+ handling.

Aldosterone response. The mineralocorticoid aldosterone contributes to potassium homeostasis. Mice with NBCe1-A deletion had significantly greater urinary aldosterone than did WT mice under both dietary conditions ($P < 0.001$ by ANOVA; Fig. 13). Urine aldosterone decreased in both WT and KO mice; the decrease was not altered by NBCe1-A deletion (P = NS by ANOVA).

Effect on ENaC expression. One mechanism through which elevated aldosterone can contribute to hypokalemia is by increasing expression of the collecting duct epithelial Na^+ channel (ENaC). However, there was no consistent effect of NBCe1-A deletion on expression of the three ENaC subunits, α, β, and γ, compared with WT mice, as assessed by immunoblot analysis (Fig. 14). We also examined the correlation of plasma K^+ with ENaC subunit expression in both WT and KO mice (Fig. 15). Serum K^+ correlated with expression of each ENaC subunit, α, β, and γ ($P < 0.001$ for α and γ and $P < 0.005$ for β, each by ANOVA). In addition, for α and γ, but not for β, there was a significant effect of NBCe1-A gene deletion ($P < 0.001$ by ANOVA). However, as shown in Fig. 15, NBCe1-A deletion decreased ENaCα and ENaCγ expression. Thus, the increased K^+ excretion observed in KO mice during hypokalemia appears unrelated to inappropriately elevated ENaC expression.

Effect on K^+ transporter expression. Hypokalemia increases expression of both α-subunits of the K^+-reabsorptive protein H^+-K^+-ATPase: HKα1 and HKα2 (16, 25, 69). However, neither HKα1 nor HKα2 expression differed between hypokalemic WT and KO mice (Table 4). Thus, the greater kaliuresis in hypokalemic KO mice than in WT mice does not appear due to decreased H^+-K^+-ATPase expression.

DISCUSSION

The present study provides important new information regarding the mechanisms effecting increased renal ammonia

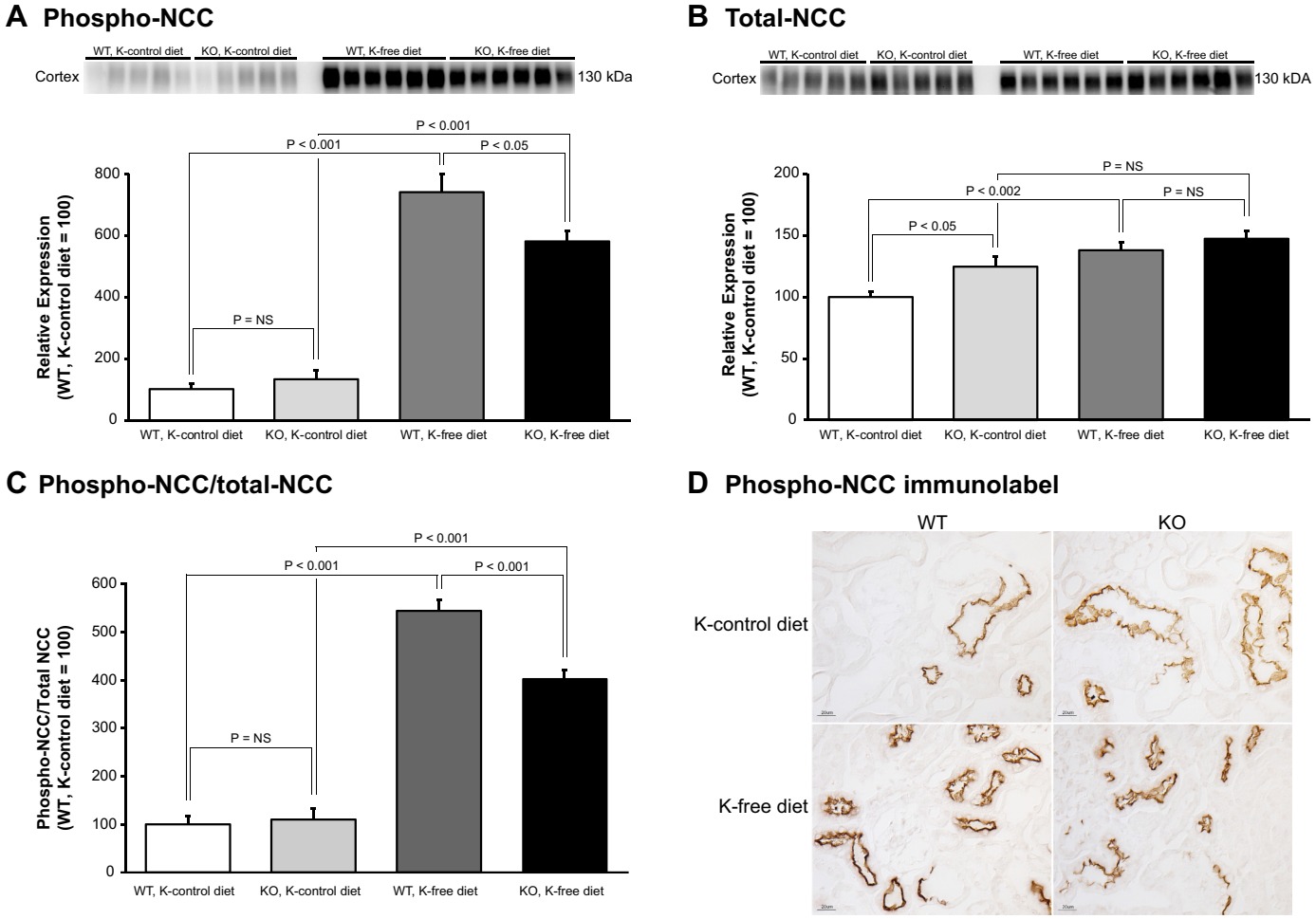

Fig. 8. Total and phospho-NaCl cotransporter response to hypokalemia. *A*: phospho-NCC expression in wild-type (WT) and Na^+-bicarbonate cotransporter electrogenic, isoform 1, splice variant A (NBCe1-A) knockout (KO) mice while on K^+ control diet and after 4 days of K^+-free diet. Phospho-NCC expression did not differ significantly between WT and KO mice while on K^+ control diet. In tissues obtained after 4 days of K^+-free diet, phospho-NCC expression increased significantly in both genotypes, but the magnitude of increase was significantly less in KO mice. *B*: total NCC response. Total NCC expression was slightly, but significantly, greater in KO mice than in WT mice while on K^+ control diet. Exposure to K^+-free diet increased total NCC expression significantly ($P < 0.001$ by ANOVA); in WT mice but not in KO mice, the increase was statistically significant, and there was no genotype effect [P = not significant (NS) by ANOVA] on the response to K^+-free diet. *C*: ratio of phospho-NCC to total NCC expression. This ratio did not differ significantly between WT and KO mice while on K^+ control diet. Exposure to K^+-free diet increased the ratio significantly in both genotypes, but the increase was significantly less in KO mice. *D*: phospho-NCC immunolabel response. Apical immunolabel intensity did not differ detectably between WT and KO mice while on K^+ control diet. Exposure to K^+-free diet for 4 days increased apical immunolabel intensity in both genotypes, but immunolabel intensity was less in KO mice than in WT mice. Images are representative of findings in 5 mice on K^+ control diet and 6 on K^+-free diet in each genotype.

excretion and potassium homeostasis during hypokalemia. First, diet-induced hypokalemia increases cortical proximal tubule NBCe1-A expression. Second, NBCe1-A is central to a hypokalemia-induced signal transduction pathway that increases urinary ammonia excretion via regulation of multiple proteins involved in proximal tubule ammonia generation. Finally, NBCe1-A expression is necessary for the maximal decrease in K^+ excretion required in response to a K^+-free diet.

The first finding in this project is that hypokalemia induced by a K^+-free diet resulted in increased NBCe1-A expression. This finding provides a mechanistic explanation for the observation that hypokalemia increases proximal tubule basolateral Na^+-coupled base exit (71). Moreover, since NBCe1-A is critical for the basolateral bicarbonate exit step required for filtered bicarbonate reabsorption and for new bicarbonate generation, the increased basolateral NBCe1-A expression likely contributes to hypokalemia's stimulation of proximal tubule bicarbonate reabsorption (37, 61).

The second major finding of these studies is that proximal tubule NBCe1-A is involved in the signaling pathway through which hypokalemia increases ammonia metabolism and excretion. Hypokalemia has multiple effects that contribute to the increased ammonia excretion. These include increased proximal tubule ammonia generation (34, 51, 54) and altered expression of several proteins involved in ammonia generation (8, 13, 32, 76). The present study shows NBCe1-A is necessary both for the increase in ammonia excretion in response to hypokalemia and for the changes in several critical proteins involved in proximal tubule ammonia generation. Blocking responses by the ammoniagenic enzymes PDG and PEPCK and the ammonia recycling protein GS likely explains the finding that NBCe1-A deletion blocked changes in ammonia excretion during hypokalemia. The observation that NBCe1-A

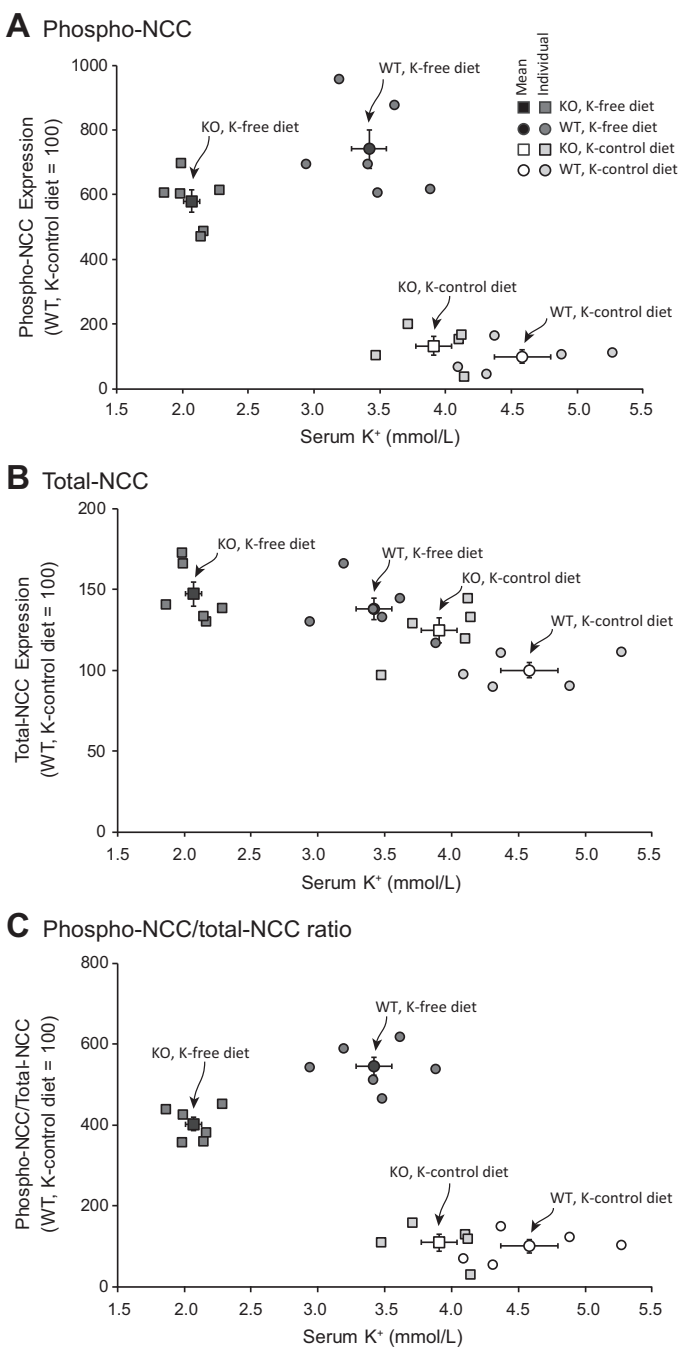

Fig. 9. Correlation of phosphorylated NaCl cotransporter (p-NCC), total (t-)NCC, and p-NCC-to-t-NCC ratio with plasma K^+ and Na^+-bicarbonate cotransporter electrogenic, isoform 1, splice variant A (NBCe1-A) genotype. *A*: p-NCC expression plotted as a function of plasma K^+ for wild-type (WT) and NBCe1-A knockout (KO) mice on K^+ control diet and K^+-free diet. Both plasma K^+ and genotype independently correlated with p-NCC expression ($P < 0.001$ for each by ANOVA). *B*: t-NCC expression relative to plasma K^+ in WT and NBCe1-A KO mice. Plasma K^+ correlated significantly with t-NCC expression ($P < 0.005$ by ANOVA), but there was no independent effect of genotype. *C*: p-NCC-to-t-NCC ratio. Both plasma K^+ and genotype were independently correlated with p-NCC-to-t-NCC ratio ($P < 0.001$ for each by ANOVA).

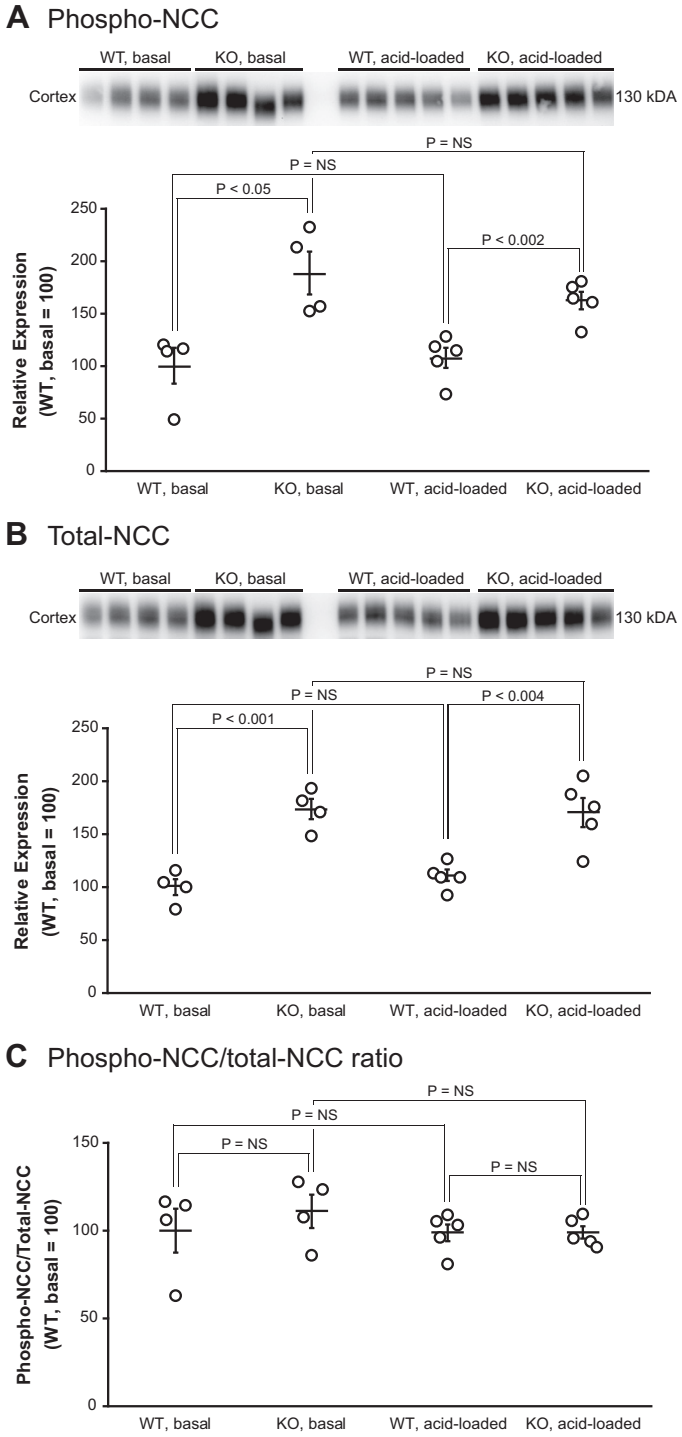

Fig. 10. Total and phospho-NaCl cotransporter (phospho-NCC) expression while on normal diet and after acid loading in wild-type (WT) and Na^+-bicarbonate cotransporter electrogenic, isoform 1, splice variant A (NBCe1-A) knockout (KO) mice. *A*: phospho-NCC expression in WT and in NBCe1-A KO mice on normal diet and after acid loading. Tissues were prepared as part of a previous work from our laboratory (45). NBCe1-A KO mice had increased phospho-NCC expression in both conditions. Acid loading did not alter phospho-NCC expression in either genotype. *B*: total NCC expression in the same mice. Total NCC expression was greater in NBCe1-A KO mice under both conditions. Acid loading did not alter total NCC expression significantly in either genotype. *C*: ratio of phospho-NCC to total NCC expression. Neither NBCe1-A KO nor acid loading altered this ratio significantly; $n = 4$ in each genotype on normal diet and 5 in each genotype on acid loading diet.

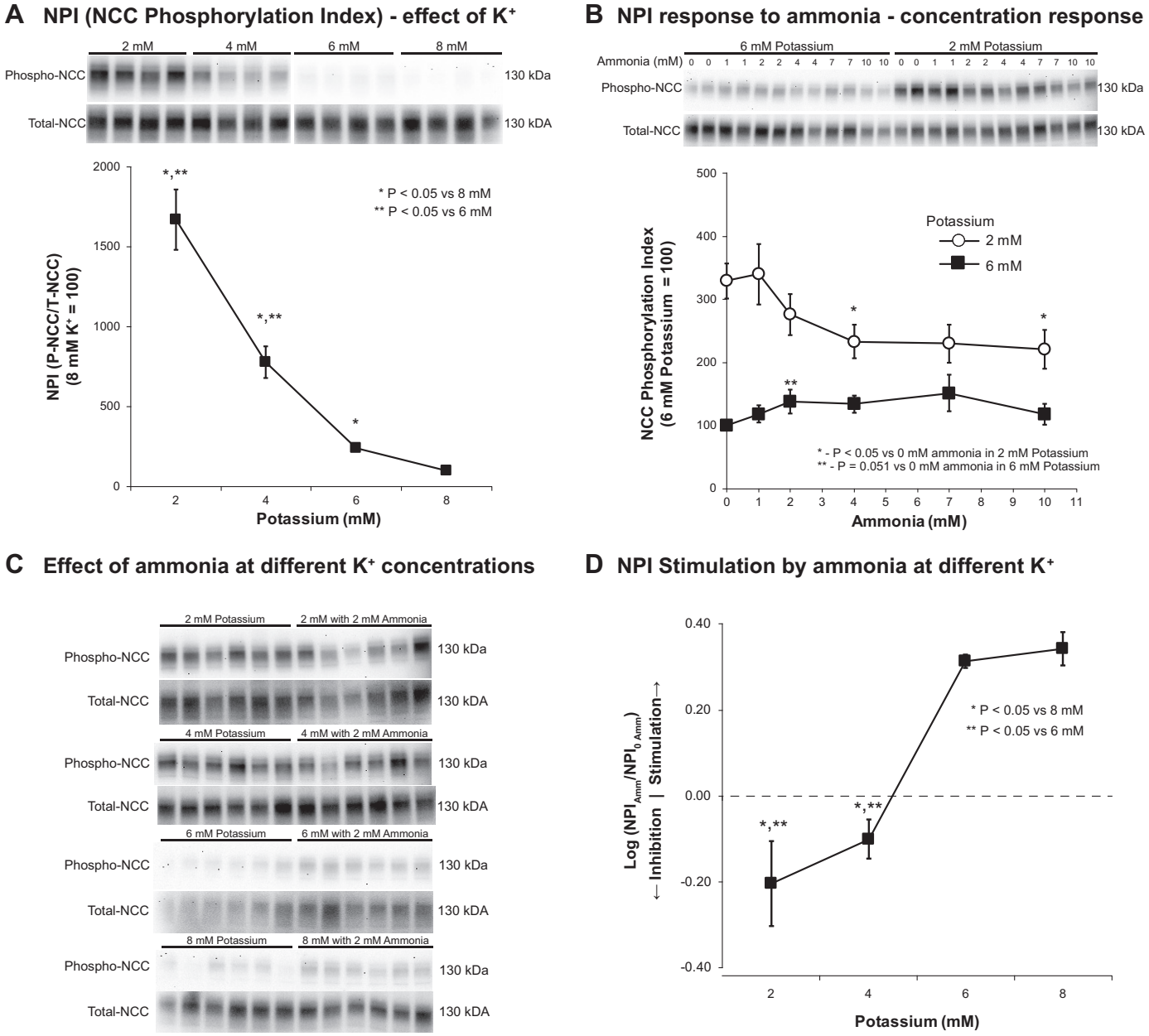

Fig. 11. NaCl cotransporter (NCC) phosphorylation index (NPI) in kidney slices. *A*: effect of media K^+ on NPI. Decreases in media K^+ stimulate NPI. *B*: effect of media ammonia on NPI when media K^+ was either 2 or 6 mM. Ammonia addition increased NPI when media K^+ was 6 mM and inhibited NPI when K^+ was 2 mM. *C*: effect of media ammonia, 2 mM, on NCC phosphorylation across a range of media K^+ concentration from 2 through 8 mM. *D*: effect of ammonia on NPI. NPI was calculated as detailed above. At each K^+ concentration, the mean of the ratio of NPI with ammonia relative to without ammonia was determined. The log of this ratio is shown, so that relative proportional changes are linearly depicted. A negative logarithm indicates ammonia decreased NPI; a positive logarithm indicates ammonia increased NPI. Each lane in the immunoblot analysis is a separate tissue section from a single kidney; results from sections exposed to the same condition are averaged and used as a single measurement for statistical analysis. Quantitative results are the mean of each kidney; $n = 4$ kidneys in each group. NPI is the mean of the of phospho-NCC-to-total NCC expression ratio. In *A* and *B*, NPI is normalized to a value of 100 in the highest media K^+ concentration solution used, as specified in the *y*-axis title.

has a critical role regulating ammonia metabolism in response to hypokalemia extends recent findings that it also has a critical role in both basal and acidosis-stimulated ammonia metabolism (45). These findings, taken together, indicate that NBCe1-A has a central role regulating proximal tubule ammonia metabolism in response to multiple stimuli.

The mechanism(s) through which NBCe1-A deletion alters the cortical proximal tubule response to hypokalemia are unknown but may involve hypokalemia-induced intracellular pH changes. In vivo measurements of renal cortical intracellular pH (pH_i), which primarily reflects proximal tubule pH_i, show that hypokalemia induces intracellular acidosis (2, 35). Because NBCe1-A is an electrogenic, bicarbonate-extruding transporter, hypokalemia-induced basolateral plasma membrane hyperpolarization would increase the electrochemical gradient for NBCe1-A-mediated bicarbonate exit; in the absence of other factors, this will decrease pH_i. Supporting this pathway is that extracellular K^+ alters proximal tubule pH_i

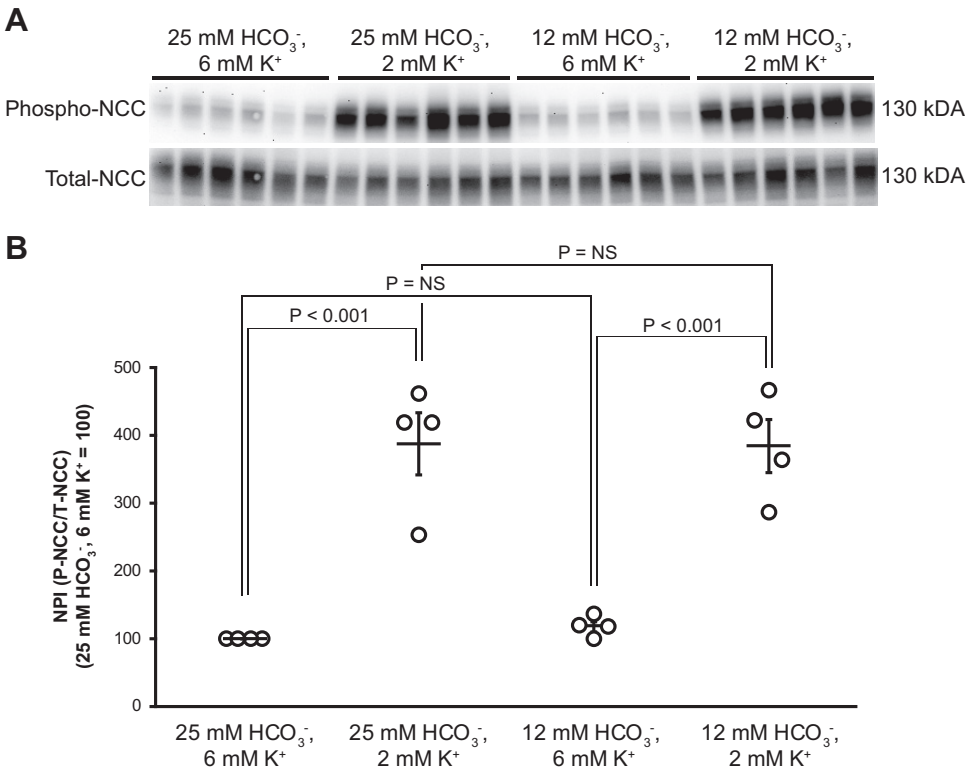

Fig. 12. Effect of altering extracellular bicarbonate on NaCl cotransporter (NCC) phosphorylation index (NPI). *A*: NCC phosphorylation and total NCC expression in tissue sections incubated with solutions containing the indicated amount of K^+ and HCO_3^-. *B*: calculated NPI under each condition. Variation in extracellular bicarbonate did not alter NPI significantly at either 2 or 6 mM potassium and did not alter significantly the increase in response to 2 mM K^+. Each lane in the immunoblot analysis is a separate tissue section from a single kidney; results from sections exposed to the same conditions are averaged and used as a single measurement for statistical analysis. Quantitative results are the mean of each kidney; $n = 4$ kidneys in each group.

through a mechanism inhibited by disulfonic stilbenes, known NBCe1-A inhibitors (67, 68). Thus, NBCe1-A deletion may blunt the intracellular acidosis response to hypokalemia. However, we cannot exclude the possibility of other mechanisms through which NBCe1-A regulates proximal tubule ammonia generation during hypokalemia.

The role of NBCe1-A in the proximal tubule ammonia response to hypokalemia is limited to cortical proximal tubule segments. This coincides with the known localization of NBCe1-A (19, 20, 45, 50, 64, 87). In contrast, in the proximal straight tubule in the outer medulla, where NBCe1-A is not present, NBCe1-A deletion did not block changes in the expression of these enzymes. Instead, in this segment, several of the responses to hypokalemia were greater in NBCe1-A KO mice than in WT mice. Either this could be an adaptive response compensating for the lack of response in the cortical proximal tubule or it could be due to the more severe hypokalemia present. One likely mechanism involves NBCe1-B, a splice variant of the SLC4A4 gene, which is expressed throughout the proximal tubule (20). A previous study has shown that metabolic acidosis increases NBCe1-B expression (20), and the present study extends this observation by showing increased expression in response to hypokalemia in NBCe1-A-null mice. In addition to increased NBCe1-B expression, there may be increased NBCe1-B activity resulting from post-translational regulation, such as an alteration in inositol 1,4,5-trisphosphate receptor-binding protein expression or in other signaling pathways that regulate NBCe1-B activity (66, 88, 89). Finally, the greater membrane hyperpolarization resulting from the more severe hypokalemia would increase the electrochemical gradient for NBCe1-B-mediated bicarbonate extrusion.

Hypokalemia increases activity or expression of several critical proteins involved in collecting duct ammonia excretion, i.e., H^+-ATPase, Rhbg, and Rhcg (5, 13, 17, 31, 39, 47, 70). However, there were no observable differences in the expression of the proteins between the hypokalemic WT and KO mice. Thus, differences in hypokalemia-stimulated ammonia excretion do not appear to be due to differences in collecting duct ammonia transport and urine acidification.

A third finding in this study is that NBCe1-A deletion altered K^+ homeostasis in response to a K^+-free diet. NBCe1-A mice provided a K^+-free diet decreased K^+ excretion less and developed more severe hypokalemia than did WT mice. Although it is tempting to attribute this response to direct effects of NBCe1-A deletion on proximal tubule K^+ transport,

Table 3. *Effect of alterations in dietary K^+ and NBCe1-A deletion on urinary 2-oxoglutarate*

	K^+-Control Diet		K^+-Free Diet	
	WT	NBCe1-A KO	WT	NBCe1-A KO
Urinary 2-oxoglutarate, μmol/day	15.4 ± 3.6 (6)	12.7 ± 2.1 (6)	1.3 ± 0.4 (6)*	1.8 ± 0.3 (6)*

Values are means ± SE. Numbers in parentheses are numbers of animals in each group. NBCe1-A KO, Na^+-bicarbonate cotransporter electrogenic, isoform 1, splice variant A knockout; WT, wild type. *$P < 0.001$ vs. the K^+ control diet for each genotype. For each diet, urinary 2-oxoglutarate did not differ significantly between WT and KO mice (P = not significant).

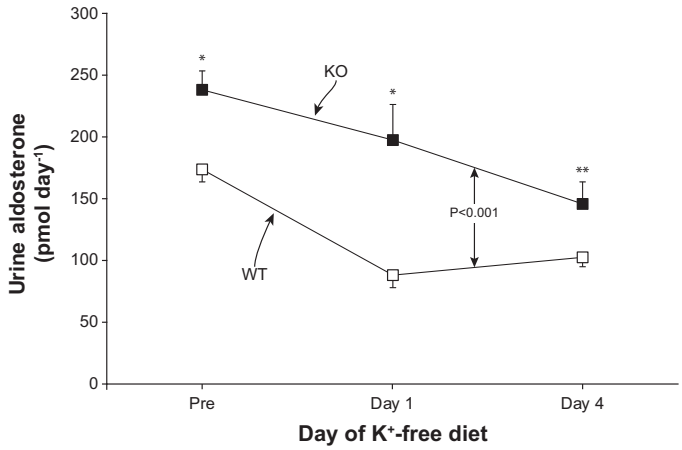

Fig. 13. Effect of Na^+-bicarbonate cotransporter electrogenic, isoform 1, splice variant A (NBCe1-A) deletion and K^+-free diet on aldosterone. Urinary aldosterone excretion was greater in NBCe1-A knockout (KO) mice than in wild-type (WT) mice under control conditions. K^+-free diet decreased urine aldosterone excretion in both WT and KO mice, and the decrease was not significantly altered by NBCe1-A deletion [P = not significant (NS) by ANOVA]; $n = 6$ in both groups at each time point.

changes in proximal tubule K^+ reabsorption do not contribute to the altered urinary K^+ during hypokalemia (49, 72). Instead, essentially all regulation of K^+ excretion results from altered distal nephron K^+ transport (49, 72).

The increased K^+ excretion during hypokalemia in NBCe1-A KO mice correlates with, and may result at least partly from, decreased NCC phosphorylation. NCC phosphorylation is necessary for transporter activity and translocation to the apical membrane. Thus, NCC phosphorylation regulates K^+ excretion by increasing electroneutral NaCl reabsorption in the DCT. This decreases the need for collecting duct Na^+ reabsorption, which is coupled to K^+ secretion (10, 75, 77). Thus, decreased NCC phosphorylation in the NBCe1-A KO mouse, shown in terms of both absolute p-NCC expression and the ratio of p-NCC to total NCC, likely contributes to the inappropriately greater urinary K^+ and the more severe hypokalemia in these mice.

The specific mechanism through which NBCe1-A deletion altered NCC phosphorylation is not identified by the present study but does not appear related to aldosterone, systemic acidosis, or effects of ammonia or of 2-oxoglutarate. Although some studies have suggested at aldosterone increases NCC phosphorylation (12, 36, 58), NBCe1-A KO mice have stimulation of aldosterone metabolism, rather than inhibition, which cannot explain the decreased phosphorylation observed. This stimulation may result from extracellular acidosis that is present (63). Diet-induced hypokalemia decreased aldosterone metabolism similarly in both genotypes, but it had quantitatively different effects on NCC phosphorylation. Thus, impaired aldosterone metabolism does not mediate the altered NCC phosphorylation. Metabolic acidosis that is present in NBCe1-A KO mice also does not appear to mediate the altered NCC phosphorylation. In the present study, we found that

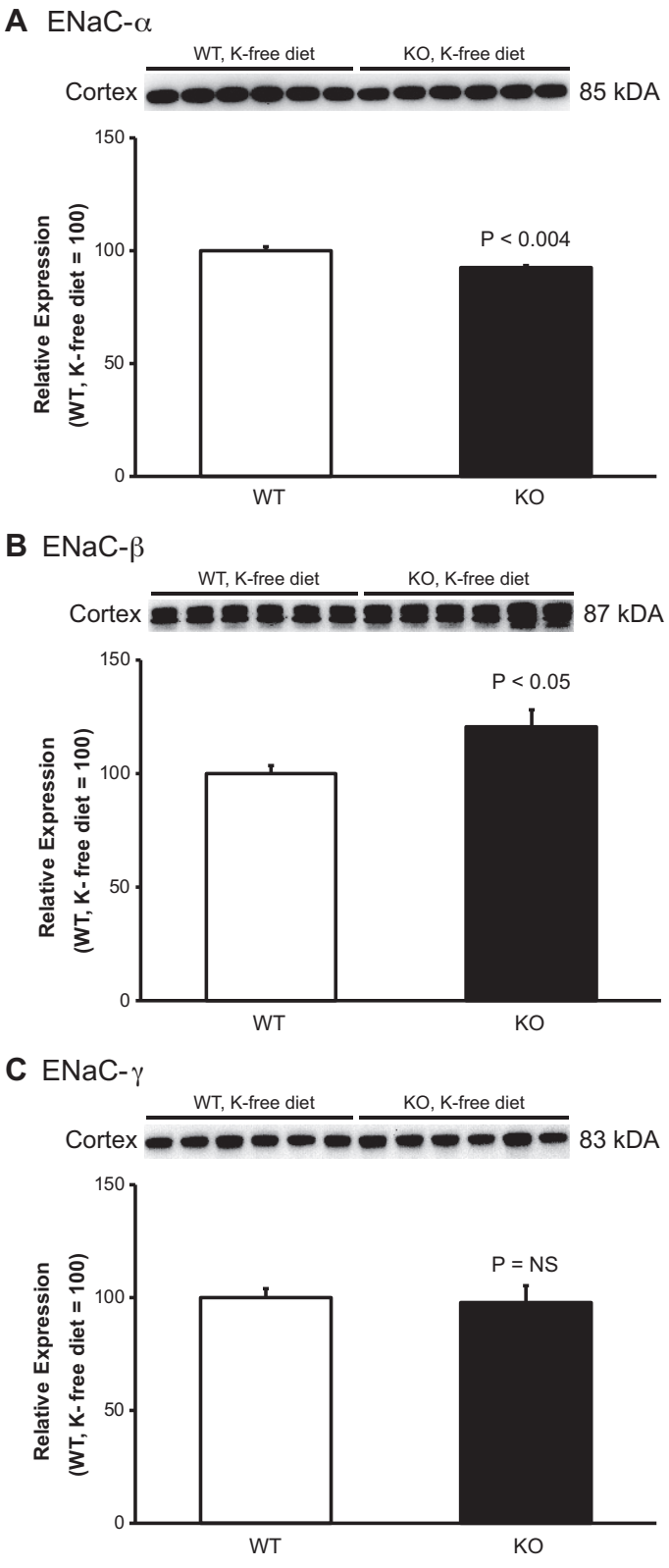

Fig. 14. Effects of Na^+-bicarbonate cotransporter electrogenic, isoform 1, splice variant A (NBCe1-A) deletion and diet-induced hypokalemia on epithelial Na^+ channel (ENaC). *A–C*: ENaCα, -β, and -γ expressions, respectively, in wild-type (WT) and NBCe1-A knockout (KO) mice on K^+-free diet. ENaCα expression was slightly but significantly decreased in KO versus WT mice; ENaCβ expression was slightly but significantly increased in KO versus WT mice; and ENaCγ expression did not differ significantly between WT and KO mice. Thus, there was no consistent effect of NBCe1-A deletion on ENaC subunit expression; $n = 6$ for each genotype.

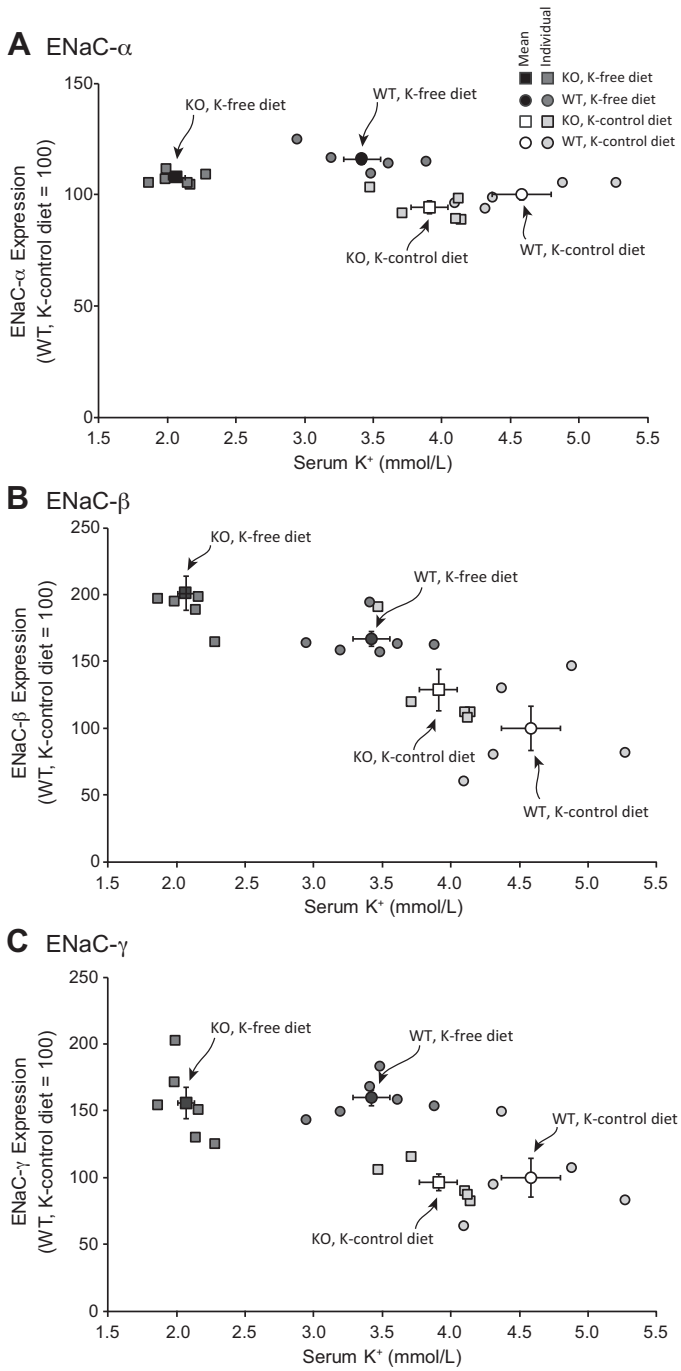

Fig. 15. Correlation of epithelial Na^+ channel (ENaC) expression with plasma K^+ in wild-type (WT) and Na^+-bicarbonate cotransporter electrogenic, isoform 1, splice variant A (NBCe1-A) knockout (KO) mice on K^+-free diet. *A*: ENaCα expression plotted as a function of plasma K^+ for WT and KO mice on K^+ control diet and K^+-free diet. Both plasma K^+ and genotype were independently correlated with ENaCα expression ($P < 0.001$ for each by ANOVA). *B*: ENaCβ expression relative to plasma K^+ in WT and NBCe1-A KO mice. Plasma K^+ correlated significantly with ENaCβ expression ($P < 0.001$ by ANOVA), but there was no independent effect of genotype. *C*: ENaCγ expression relative to plasma K^+. Both plasma K^+ and genotype were independently correlated with ENaCγ expression ($P < 0.001$ for each by ANOVA).

Table 4. *H^+-K^+-ATPase α-subunit expression in mice on K^+-free diet*

Parameter	WT	NBCe1-A KO	*P* Value
HKα1	100 ± 19 (4)	111 ± 24 (3)	NS
HKα2	100 ± 23 (4)	158 ± 32 (3)	NS

Values are means ± SE. Numbers in parentheses are numbers of animals in each group. NBCe1-A KO, Na^+-bicarbonate cotransporter electrogenic, isoform 1, splice variant A knockout; WT, wild type; NS, not significant. Expression relative to GAPDH is normalized for each H^+-K^+-ATPase (HK) α-subunit such that mean expression in WT mice = 100.0.

acid-loading WT mice did not alter NCC phosphorylation. Another study found that metabolic acidosis induced by oral NH_4Cl administration, a different model of acidosis, increased total NCC and p-NCC expression but concluded that this resulted from the natriuretic response in that model and not the acidosis itself (21). Thus, the present study is consistent with the conclusion in Ref. 21 and supports the interpretation that the impaired NCC phosphorylation seen in NBCe1-A KO mice with diet-induced hypokalemia is unrelated to the concomitant acidosis.

We also considered the possibility that altered ammonia metabolism could explain the findings. At low extracellular K^+ concentrations, ammonia inhibited NPI, indicating that impaired ammonia generation in hypokalemic NBCe1-A KO mice could not explain the decreased NCC phosphorylation observed. It is interesting to note that, at relatively high extracellular K^+, 6 and 8 mM, ammonia stimulated NCC phosphorylation, whereas ammonia blunted NCC phosphorylation with 2 and 4 mM K^+. Thus, balanced around an extracellular K^+ of ~5 mM, ammonia blunts the effects of extracellular K^+ to alter NPI. One possible explanation for this observation is that extracellular NH_4^+ acts as a partial antagonist of basolateral $K_{ir}4.1/K_{ir}5.1$ K^+ conductance. Supporting this possibility is the observation that NH_4^+ and K^+ have nearly identical biophysical characteristics and that previous studies have suggested that essentially all K^+-transporting proteins have a partial affinity for NH_4^+ (14, 80, 82).

Another mechanism that may contribute to the inappropriate kaliuresis observed in NBCe1-A KO mice during diet-induced hypokalemia may involve impaired ammonia metabolism. Previous studies, performed in both humans and rodents, have shown that acutely increasing ammonia production, with exogenous glutamine administration, decreases urinary K^+ excretion with a time course identical to the increased ammonia excretion and that these changes occur independently of extracellular K^+ (34, 74). Studies that examined the nephron site of this response identified that this response involved altered K^+ transport in the distal nephron (34), and microperfusion studies have shown that ammonia inhibits cortical collecting duct net and unidirectional K^+ secretion (28) and acutely increases H^+-K^+-ATPase activity (22–24). Ammonia's inhibition of unidirectional K^+ secretion may result from its inhibition of ENaC (52). Ammonia's stimulation of H^+-K^+-ATPase occurs rapidly, within 30 min, is independent of pH_i and involves microtubule-dependent, intracellular Ca^{+2}-dependent mechanisms (22–24). Thus, ammonia may serve as a signaling molecule, produced in the proximal tubule in response to hypokalemia through a NBCe1-A-dependent pathway that regulates distal nephron K^+ transport. Another possibility is that

differences in distal nephron flow rates resulting from proximal tubule NBCe1-A deletion induce differences in flow-stimulated K^+ secretion. Against this possibility is that urine volume did not differ significantly between WT and KO mice on the K^+-free diet (data not shown). Finally, we cannot exclude the possibility that impaired proximal tubule NaCl reabsorption, possibly resulting from NBCe1-A deletion, leads to increased collecting duct Na^+ delivery, which also increases collecting duct K^+ secretion.

This study also reports the effect of NBCe1-A deletion on the intrarenal signaling molecule, 2-oxoglutarate. 2-Oxoglutarate excretion decreases in response to metabolic acidosis (3). The present study shows, for the first time to our knowledge, that 2-oxoglutarate excretion is also regulated in response to hypokalemia. Moreover, this effect occurs in both WT and KO mice, and there is no effect of NBCe1-A deletion on this response. Thus, NBCe1-A appears unlikely to have a major role in the effect of hypokalemia on 2-oxoglutarate excretion. This could reflect NBCe1-A having no role in proximal tubule 2-oxoglutarate metabolism, that a major component of hypokalemia-induced alterations in 2-oxoglutarate occur downstream of the cortical proximal tubule, or that there are adaptive responses to NBCe1-A deletion that compensate for its absence.

Unstimulated NBCe1-A KO mice exhibited mild hypokalemia in the present study, but not in our previous study (45). This difference correlates with differences in NCC phosphorylation: p-NCC was greater in KO mice than in WT mice while on normal rodent chow (Fig. 10, present study) but not while on K^+ control diet (Fig. 8, present study). The difference may relate to different basal diets used in the two studies. In the present study, the basal diet was a "K^+ control diet," which is a semisynthetic diet designed to match the K^+-free diet with the exception of the K content. In our other study (45), the basal diet was normal rodent chow. Thus, we propose that unexplained differences in these two diets leads to differences in NCC phosphorylation that alters the maintenance of normal serum K^+.

In summary, the present study provides important new information regarding the renal response to hypokalemia. NBCe1-A, an integral basolateral plasma membrane protein, increases in response to diet-induced hypokalemia, is essential to the mechanism through which hypokalemia increases ammonia excretion, and does so by regulating the cortical proximal tubule expression of key enzymes involved in ammonia generation in response to diet-induced hypokalemia. Second, NBCe1-A is critical to the pathway by which renal K^+ excretion maximally decreases in response to diet-induced hypokalemia. This is due in part to the dependency of normal hypokalemia-induced stimulation of NCC phosphorylation on NBCe1-A expression. It may also result, at least in part, from the decreased ammonia metabolism leading to decreased effects of ammonia on collecting duct K^+ secretion and reabsorption.

ACKNOWLEDGMENTS

We thank Ram Khattri, PhD, and Matthew E. Merritt, PhD, for measuring 2-oxoglutarate.

GRANTS

This work was supported by National Institutes of Health (NIH) Grants R01 DK-045788, R01 DK-107798, 5T32 DK-104721, R01 DK-110375, 49K08 DK-120873, and R01 DK-054231 and the Foundation LeDucq. The 2-oxoglutarate measurements were performed in the McKnight Brain Institute at the National High Magnetic Field Laboratory's Advanced Magnetic Resonance Imaging and Spectroscopy Facility, which is supported by National Science Foundation Cooperative Agreement DMR-1157490* and State of Florida Grants DMR-1157490 and DMR-1644779. These measurements were also supported, in part, by NIH Grant S10-RR-031637 for magnetic resonance instrumentation and NIH Grant U24-DK-097209 for NMR data analysis.

DISCLAIMERS

The findings and conclusions in this paper do not reflect official opinions of the United States Department of Veterans Affairs.

DISCLOSURES

No conflicts of interest, financial or otherwise, are declared by the author(s).

AUTHOR CONTRIBUTIONS

H.-W.L., J.W.V., and I.D.W. conceived and designed research; H.-W.L., A.N.H., M.F.R., and C.S.W. performed experiments; H.-W.L., A.N.H., J.W.V., and I.D.W. analyzed data; A.N.H., J.W.V., and I.D.W. interpreted results of experiments; H.-W.L. and I.D.W. prepared figures; I.D.W. drafted manuscript; H.-W.L., A.N.H., M.F.R., P.A.W., C.S.W., J.W.V., and I.D.W. edited and revised manuscript; H.-W.L., A.N.H., P.A.W., C.S.W., J.W.V., and I.D.W. approved final version of manuscript.

REFERENCES

1. **Aalkjaer C, Frische S, Leipziger J, Nielsen S, Praetorius J.** Sodium coupled bicarbonate transporters in the kidney, an update. *Acta Physiol Scand* 181: 505–512, 2004. doi:10.1111/j.1365-201X.2004.01324.x.
2. **Adam WR, Koretsky AP, Weiner MW.** ^{31}P-NMR in vivo measurement of renal intracellular pH: effects of acidosis and K^+ depletion in rats. *Am J Physiol Renal Physiol* 251: F904–F910, 1986. doi:10.1152/ajprenal.1986.251.5.F904.
3. **Balagura S, Pitts RF.** Renal handling of α-ketoglutarate by the dog. *Am J Physiol* 207: 483–494, 1964. doi:10.1152/ajplegacy.1964.207.2.483.
4. **Bazúa-Valenti S, Gamba G.** Revisiting the NaCl cotransporter regulation by with-no-lysine kinases. *Am J Physiol Cell Physiol* 308: C779–C791, 2015. doi:10.1152/ajpcell.00065.2015.
5. **Bishop JM, Lee HW, Handlogten ME, Han KH, Verlander JW, Weiner ID.** Intercalated cell-specific Rh B glycoprotein deletion diminishes renal ammonia excretion response to hypokalemia. *Am J Physiol Renal Physiol* 304: F422–F431, 2013. doi:10.1152/ajprenal.00301.2012.
6. **Bishop JM, Verlander JW, Lee HW, Nelson RD, Weiner AJ, Handlogten ME, Weiner ID.** Role of the Rhesus glycoprotein, Rh B glycoprotein, in renal ammonia excretion. *Am J Physiol Renal Physiol* 299: F1065–F1077, 2010. doi:10.1152/ajprenal.00277.2010.
7. **Bourgeois S, Bounoure L, Mouro-Chanteloup I, Colin Y, Brown D, Wagner CA.** The ammonia transporter RhCG modulates urinary acidification by interacting with the vacuolar proton-ATPases in renal intercalated cells. *Kidney Int* 93: 390–402, 2018. doi:10.1016/j.kint.2017.07.027.
8. **Busque SM, Wagner CA.** Potassium restriction, high protein intake, and metabolic acidosis increase expression of the glutamine transporter SNAT3 (Slc38a3) in mouse kidney. *Am J Physiol Renal Physiol* 297: F440–F450, 2009. doi:10.1152/ajprenal.90318.2008.
9. **Capasso G, Kinne R, Malnic G, Giebisch G.** Renal bicarbonate reabsorption in the rat. I. Effects of hypokalemia and carbonic anhydrase. *J Clin Invest* 78: 1558–1567, 1986. doi:10.1172/JCI112748.
10. **Castañeda-Bueno M, Cervantes-Perez LG, Rojas-Vega L, Arroyo-Garza I, Vázquez N, Moreno E, Gamba G.** Modulation of NCC activity by low and high K(+) intake: insights into the signaling pathways involved. *Am J Physiol Renal Physiol* 306: F1507–F1519, 2014. doi:10.1152/ajprenal.00255.2013.
11. **Chan YL, Biagi B, Giebisch G.** Control mechanisms of bicarbonate transport across the rat proximal convoluted tubule. *Am J Physiol Renal Physiol* 242: F532–F543, 1982. doi:10.1152/ajprenal.1982.242.5.F532.
12. **Cheng L, Poulsen SB, Wu Q, Esteva-Font C, Olesen ETB, Peng L, Olde B, Leeb-Lundberg LMF, Pisitkun T, Rieg T, Dimke H, Fenton RA.** Rapid aldosterone-mediated signaling in the DCT increases activity of the thiazide-sensitive NaCl cotransporter. *J Am Soc Nephrol* 30: 1454–1470, 2019. doi:10.1681/ASN.2018101025.
13. **Cheval L, Duong Van Huyen JP, Bruneval P, Verbavatz JM, Elalouf JM, Doucet A.** Plasticity of mouse renal collecting duct in response to

potassium depletion. *Physiol Genomics* 19: 61–73, 2004. doi:10.1152/physiolgenomics.00055.2004.
14. **Choe H, Sackin H, Palmer LG.** Permeation properties of inward-rectifier potassium channels and their molecular determinants. *J Gen Physiol* 115: 391–404, 2000. doi:10.1085/jgp.115.4.391.
15. **Conjard A, Komaty O, Delage H, Boghossian M, Martin M, Ferrier B, Baverel G.** Inhibition of glutamine synthetase in the mouse kidney: a novel mechanism of adaptation to metabolic acidosis. *J Biol Chem* 278: 38159–38166, 2003. doi:10.1074/jbc.M302885200.
16. **Doucet A.** H^+,K^+-ATPASE in the kidney: localization and function in the nephron. *Exp Nephrol* 5: 271–276, 1997.
17. **DuBose TD Jr, Gitomer J, Codina J.** H^+,K^+-ATPase. *Curr Opin Nephrol Hypertens* 8: 597–602, 1999. doi:10.1097/00041552-199909000-00011.
18. **Eliel LP, Pearson OH, White FC.** Postoperative potassium deficit and metabolic alkalosis; the pathogenic significance of operative trauma and of potassium and phosphorus deprivation. *J Clin Invest* 31: 419–432, 1952. doi:10.1172/JCI102625.
19. **Endo Y, Yamazaki S, Moriyama N, Li Y, Ariizumi T, Kudo A, Kawakami H, Tanaka Y, Horita S, Yamada H, Seki G, Fujita T.** Localization of NBC1 variants in rat kidney. *Nephron Physiol* 104: p87–94, 2006. doi:10.1159/000094003.
20. **Fang L, Lee H-W, Chen C, Harris AN, Romero MF, Verlander JW, Weiner ID.** Expression of the B splice variant of NBCe1 (SLC4A4) in the mouse kidney. *Am J Physiol Renal Physiol* 315: F417–F428, 2018. doi:10.1152/ajprenal.00515.2017.
21. **Fang YW, Yang SS, Cheng CJ, Tseng MH, Hsu HM, Lin SH.** Chronic metabolic acidosis activates renal tubular sodium chloride cotransporter through angiotension II-dependent WNK4-SPAK phosphorylation pathway. *Sci Rep* 6: 18360, 2016. doi:10.1038/srep18360.
22. **Frank AE, Weiner ID.** Effects of ammonia on acid-base transport by the B-type intercalated cell. *J Am Soc Nephrol* 12: 1607–1614, 2001.
23. **Frank AE, Wingo CS, Andrews PM, Ageloff S, Knepper MA, Weiner ID.** Mechanisms through which ammonia regulates cortical collecting duct net proton secretion. *Am J Physiol Renal Physiol* 282: F1120–F1128, 2002. doi:10.1152/ajprenal.00266.2001.
24. **Frank AE, Wingo CS, Weiner ID.** Effects of ammonia on bicarbonate transport in the cortical collecting duct. *Am J Physiol Renal Physiol* 278: F219–F226, 2000. doi:10.1152/ajprenal.2000.278.2.F219.
25. **Greenlee MM, Lynch IJ, Gumz ML, Cain BD, Wingo CS.** The renal H,K-ATPases. *Curr Opin Nephrol Hypertens* 19: 478–482, 2010. doi:10.1097/MNH.0b013e32833ce65f.
26. **Grimm PR, Lazo-Fernandez Y, Delpire E, Wall SM, Dorsey SG, Weinman EJ, Coleman R, Wade JB, Welling PA.** Integrated compensatory network is activated in the absence of NCC phosphorylation. *J Clin Invest* 125: 2136–2150, 2015. doi:10.1172/JCI78558.
27. **Hadchouel J, Ellison DH, Gamba G.** Regulation of renal electrolyte transport by WNK and SPAK-OSR1 Kinases. *Annu Rev Physiol* 78: 367–389, 2016. doi:10.1146/annurev-physiol-021115-105431.
28. **Hamm LL, Gillespie C, Klahr S.** NH_4Cl inhibition of transport in the rabbit cortical collecting tubule. *Am J Physiol Renal Physiol* 248: F631–F637, 1985. doi:10.1152/ajprenal.1985.248.5.F631.
29. **Han KH, Croker BP, Clapp WL, Werner D, Sahni M, Kim J, Kim HY, Handlogten ME, Weiner ID.** Expression of the ammonia transporter, rh C glycoprotein, in normal and neoplastic human kidney. *J Am Soc Nephrol* 17: 2670–2679, 2006. doi:10.1681/ASN.2006020160.
30. **Han K-H, Lee HW, Handlogten ME, Whitehill F, Osis G, Croker BP, Clapp WL, Verlander JW, Weiner ID.** Expression of the ammonia transporter family member, Rh B glycoprotein, in the human kidney. *Am J Physiol Renal Physiol* 304: F972–F981, 2013. doi:10.1152/ajprenal.00550.2012.
31. **Han KH, Lee HW, Handlogten ME, Bishop JM, Levi M, Kim J, Verlander JW, Weiner ID.** Effect of hypokalemia on renal expression of the ammonia transporter family members, Rh B glycoprotein and Rh C glycoprotein, in the rat kidney. *Am J Physiol Renal Physiol* 301: F823–F832, 2011. doi:10.1152/ajprenal.00266.2011.
32. **Abu Hossain S, Chaudhry FA, Zahedi K, Siddiqui F, Amlal H.** Cellular and molecular basis of increased ammoniagenesis in potassium deprivation. *Am J Physiol Renal Physiol* 301: F969–F978, 2011. doi:10.1152/ajprenal.00010.2011.
33. **Iacobellis M, Muntwyler E, Griffin GE.** Enzyme concentration changes in the kidneys of protein- and/or potassium-deficient rats. *Am J Physiol* 178: 477–482, 1954. doi:10.1152/ajplegacy.1954.178.3.477.
34. **Jaeger P, Karlmark B, Giebisch G.** Ammonium transport in rat cortical tubule: relationship to potassium metabolism. *Am J Physiol Renal Physiol* 245: F593–F600, 1983. doi:10.1152/ajprenal.1983.245.5.F593.
35. **Jones B, Simpson DP.** Influence of alterations in acid-base conditions on intracellular pH of intact renal cortex. *Ren Physiol* 6: 28–35, 1983. doi:10.1159/000172878.
36. **Ko B, Mistry AC, Hanson L, Mallick R, Wynne BM, Thai TL, Bailey JL, Klein JD, Hoover RS.** Aldosterone acutely stimulates NCC activity via a SPAK-mediated pathway. *Am J Physiol Renal Physiol* 305: F645–F652, 2013. doi:10.1152/ajprenal.00053.2013.
37. **Kunau RT Jr, Frick A, Rector FC Jr, Seldin DW.** Micropuncture study of the proximal tubular factors responsible for the maintenance of alkalosis during potassium deficiency in the rat. *Clin Sci* 34: 223–231, 1968.
38. **Kurtz I, Zhu Q.** Structure, function, and regulation of the SLC4 NBCe1 transporter and its role in causing proximal renal tubular acidosis. *Curr Opin Nephrol Hypertens* 22: 572–583, 2013. doi:10.1097/MNH.0b013e328363ff43.
39. **Laroche-Joubert N, Doucet A.** Collecting duct adaptation to potassium depletion. *Semin Nephrol* 19: 390–398, 1999.
40. **Lee HW, Handlogten ME, Osis G, Clapp WL, Wakefield DN, Verlander JW, Weiner ID.** Expression of sodium-dependent dicarboxylate transporter 1 (NaDC1/SLC13A2) in normal and neoplastic human kidney. *Am J Physiol Renal Physiol* 312: F427–F435, 2017. doi:10.1152/ajprenal.00559.2016.
41. **Lee HW, Verlander JW, Bishop JM, Igarashi P, Handlogten ME, Weiner ID.** Collecting duct-specific Rh C glycoprotein deletion alters basal and acidosis-stimulated renal ammonia excretion. *Am J Physiol Renal Physiol* 296: F1364–F1375, 2009. doi:10.1152/ajprenal.90667.2008.
42. **Lee HW, Osis G, Handlogten ME, Guo H, Verlander JW, Weiner ID.** Effect of dietary protein restriction on renal ammonia metabolism. *Am J Physiol Renal Physiol* 308: F1463–F1473, 2015. doi:10.1152/ajprenal.00077.2015.
43. **Lee HW, Osis G, Handlogten ME, Lamers WH, Chaudhry FA, Verlander JW, Weiner ID.** Proximal tubule-specific glutamine synthetase deletion alters basal and acidosis-stimulated ammonia metabolism. *Am J Physiol Renal Physiol* 310: F1229–F1242, 2016. doi:10.1152/ajprenal.00547.2015.
44. **Lee HW, Osis G, Handlogten ME, Verlander JW, Weiner ID.** Proximal tubule glutamine synthetase expression is necessary for the normal response to dietary protein restriction. *Am J Physiol Renal Physiol* 313: F116–F125, 2017. doi:10.1152/ajprenal.00048.2017.
45. **Lee HW, Osis G, Harris AN, Fang L, Romero MF, Handlogten ME, Verlander JW, Weiner ID.** NBCe1-A regulates proximal tubule ammonia metabolism under basal conditions and in response to metabolic acidosis. *J Am Soc Nephrol* 29: 1182–1197, 2018. doi:10.1681/ASN.2017080935.
46. **Lee HW, Verlander JW, Bishop JM, Nelson RD, Handlogten ME, Weiner ID.** Effect of intercalated cell-specific Rh C glycoprotein deletion on basal and metabolic acidosis-stimulated renal ammonia excretion. *Am J Physiol Renal Physiol* 299: F369–F379, 2010. doi:10.1152/ajprenal.00120.2010.
47. **Lee HW, Verlander JW, Bishop JM, Handlogten ME, Han KH, Weiner ID.** Renal ammonia excretion in response to hypokalemia: effect of collecting duct-specific Rh C glycoprotein deletion. *Am J Physiol Renal Physiol* 304: F410–F421, 2013. doi:10.1152/ajprenal.00300.2012.
48. **Lee HW, Verlander JW, Handlogten ME, Han K-H, Weiner ID.** Effect of collecting duct-specific deletion of both Rh B glycoprotein (Rhbg) and Rh C glycoprotein (Rhcg) on renal response to metabolic acidosis. *Am J Physiol Renal Physiol* 306: F389–F400, 2014. doi:10.1152/ajprenal.00176.2013.
49. **Malnic G, Klose RM, Giebisch G.** Micropuncture study of renal potassium excretion in the rat. *Am J Physiol* 206: 674–686, 1964. doi:10.1152/ajplegacy.1964.206.4.674.
50. **Maunsbach AB, Vorum H, Kwon TH, Nielsen S, Simonsen B, Choi I, Schmitt BM, Boron WF, Aalkjaer C.** Immunoelectron microscopic localization of the electrogenic $Na/HCO_{(3)}$ cotransporter in rat and ambystoma kidney. *J Am Soc Nephrol* 11: 2179–2189, 2000.
51. **Nagami GT.** Effect of bath and luminal potassium concentration on ammonia production and secretion by mouse proximal tubules perfused in vitro. *J Clin Invest* 86: 32–39, 1990. doi:10.1172/JCI114702.
52. **Nakhoul NL, Hering-Smith KS, Abdulnour-Nakhoul SM, Hamm LL.** Ammonium interaction with the epithelial sodium channel. *Am J Physiol*

Renal Physiol 281: F493–F502, 2001. doi:10.1152/ajprenal.2001.281.3.F493.

53. **Nakhoul NL, Lee Hamm L.** Characteristics of mammalian Rh glycoproteins (SLC42 transporters) and their role in acid-base transport. *Mol Aspects Med* 34: 629–637, 2013. doi:10.1016/j.mam.2012.05.013.
54. **Nonoguchi H, Takehara Y, Endou H.** Intra- and inter-nephron heterogeneity of ammoniagenesis in rats: effects of chronic metabolic acidosis and potassium depletion. *Pflugers Arch* 407: 245–251, 1986. doi:10.1007/BF00585298.
55. **Osis G, Handlogten ME, Lee H-W, Hering-Smith KS, Huang W, Romero MF, Verlander JW, Weiner ID.** Effect of NBCe1 deletion on renal citrate and 2-oxoglutarate handling. *Physiol Rep* 4: e12778, 2016. doi:10.14814/phy2.12778.
56. **Parker MD, Boron WF.** The divergence, actions, roles, and relatives of sodium-coupled bicarbonate transporters. *Physiol Rev* 93: 803–959, 2013. doi:10.1152/physrev.00023.2012.
57. **Peti-Peterdi J.** Mitochondrial TCA cycle intermediates regulate body fluid and acid-base balance. *J Clin Invest* 123: 2788–2790, 2013. doi:10.1172/JCI68095.
58. **Poulsen SB, Christensen BM.** Long-term aldosterone administration increases renal Na^+-Cl^- cotransporter abundance in late distal convoluted tubule. *Am J Physiol Renal Physiol* 313: F756–F766, 2017. doi:10.1152/ajprenal.00352.2016.
59. **Ransick A, Lindstrom NO, Liu J, Qin Z, Guo J-J, Alvarado GF, Kim AD, Black HG, Kim J, McMahon AP.** Single cell profiling reveals sex, lineage and regional diversity in the mouse kidney. *rxivist* 51: 399–413.e7, 2019. doi:10.1016/j.devcel.2019.10.005.
60. **Ravanbakhsh S, Liu P, Bjorndahl TC, Mandal R, Grant JR, Wilson M, Eisner R, Sinelnikov I, Hu X, Luchinat C, Greiner R, Wishart DS.** Accurate, fully-automated NMR spectral profiling for metabolomics. *PLoS One* 10: e0124219, 2015. [Erratum in *PLoS One* 10: e0132873, 2015.] doi:10.1371/journal.pone.0124219.
61. **Rector FC Jr, Bloomer HA, Seldin DW.** Effect of potassium deficiency on the reabsorption of bicarbonate in the proximal tubule of the rat kidney. *J Clin Invest* 43: 1976–1982, 1964. doi:10.1172/JCI105071.
62. **Rodan AR, Cheng CJ, Huang CL.** Recent advances in distal tubular potassium handling. *Am J Physiol Renal Physiol* 300: F821–F827, 2011. doi:10.1152/ajprenal.00742.2010.
63. **Schambelan M, Sebastian A, Katuna BA, Arteaga E.** Adrenocortical hormone secretory response to chronic NH_4Cl-induced metabolic acidosis. *Am J Physiol Endocrinol Physiol* 252: E454–E460, 1987. doi:10.1152/ajpendo.1987.252.4.E454.
64. **Schmitt BM, Biemesderfer D, Romero MF, Boulpaep EL, Boron WF.** Immunolocalization of the electrogenic Na^+-HCO^-_3 cotransporter in mammalian and amphibian kidney. *Am J Physiol Renal Physiol* 276: F27–F38, 1999. doi:10.1152/ajprenal.1999.276.1.F27.
65. **Seldin DW, Rector FC Jr.** Symposium on acid-base homeostasis. The generation and maintenance of metabolic alkalosis. *Kidney Int* 1: 306–321, 1972. doi:10.1038/ki.1972.43.
66. **Shirakabe K, Priori G, Yamada H, Ando H, Horita S, Fujita T, Fujimoto I, Mizutani A, Seki G, Mikoshiba K.** IRBIT, an inositol 1,4,5-trisphosphate receptor-binding protein, specifically binds to and activates pancreas-type Na^+/HCO^-_3 cotransporter 1 (pNBC1). *Proc Natl Acad Sci USA* 103: 9542–9547, 2006. doi:10.1073/pnas.0602250103.
67. **Siebens AW, Boron WF.** Depolarization-induced alkalinization in proximal tubules. I. Characteristics and dependence on Na^+. *Am J Physiol Renal Physiol* 256: F342–F353, 1989. doi:10.1152/ajprenal.1989.256.2.F342.
68. **Siebens AW, Boron WF.** Depolarization-induced alkalinization in proximal tubules. II. Effects of lactate and SITS. *Am J Physiol Renal Physiol* 256: F354–F365, 1989. doi:10.1152/ajprenal.1989.256.2.F354.
69. **Silver RB, Soleimani M.** H^+-K^+-ATPases: regulation and role in pathophysiological states. *Am J Physiol Renal Physiol* 276: F799–F811, 1999. doi:10.1152/ajprenal.1999.276.6.F799.
70. **Silver RB, Breton S, Brown D.** Potassium depletion increases proton pump (H^+-ATPase) activity in intercalated cells of cortical collecting duct. *Am J Physiol Renal Physiol* 279: F195–F202, 2000. doi:10.1152/ajprenal.2000.279.1.F195.
71. **Soleimani M, Bergman JA, Hosford MA, McKinney TD.** Potassium depletion increases luminal Na^+/H^+ exchange and basolateral Na^+:$CO_3^=$:HCO^-_3 cotransport in rat renal cortex. *J Clin Invest* 86: 1076–1083, 1990. doi:10.1172/JCI114810.
72. **Stanton BA, Giebisch GH.** Renal potassium tgransport. *Compr Physiol* 25: 813–874, 2011.
73. **Tannen RL.** The effect of uncomplicated potassium depletion on urine acidification. *J Clin Invest* 49: 813–827, 1970. doi:10.1172/JCI106295.
74. **Tannen RL, Terrien T.** Potassium-sparing effect of enhanced renal ammonia production. *Am J Physiol* 228: 699–705, 1975. doi:10.1152/ajplegacy.1975.228.3.699.
75. **Terker AS, Zhang C, Erspamer KJ, Gamba G, Yang CL, Ellison DH.** Unique chloride-sensing properties of WNK4 permit the distal nephron to modulate potassium homeostasis. *Kidney Int* 89: 127–134, 2016. doi:10.1038/ki.2015.289.
76. **Verlander JW, Chu D, Lee HW, Handlogten ME, Weiner ID.** Expression of glutamine synthetase in the mouse kidney: localization in multiple epithelial cell types and differential regulation by hypokalemia. *Am J Physiol Renal Physiol* 305: F701–F713, 2013. doi:10.1152/ajprenal.00030.2013.
77. **Wade JB, Liu J, Coleman R, Grimm PR, Delpire E, Welling PA.** SPAK-mediated NCC regulation in response to low-K^+ diet. *Am J Physiol Renal Physiol* 308: F923–F931, 2015. doi:10.1152/ajprenal.00388.2014.
78. **Wagner CA, Devuyst O, Bourgeois S, Mohebbi N.** Regulated acid-base transport in the collecting duct. *Pflugers Arch* 458: 137–156, 2009. doi:10.1007/s00424-009-0657-z.
79. **Weiner ID.** Roles of renal ammonia metabolism other than in acid-base homeostasis. *Pediatr Nephrol* 32: 933–942, 2017. doi:10.1007/s00467-016-3401-x.
80. **Weiner ID, Hamm LL.** Molecular mechanisms of renal ammonia transport. *Annu Rev Physiol* 69: 317–340, 2007. doi:10.1146/annurev.physiol.69.040705.142215.
81. **Weiner ID, Mitch WE, Sands JM.** Urea and ammonia metabolism and the control of renal nitrogen excretion. *Clin J Am Soc Nephrol* 10: 1444–1458, 2015. doi:10.2215/CJN.10311013.
82. **Weiner ID, Verlander JW.** Role of NH3 and NH^+_4 transporters in renal acid-base transport. *Am J Physiol Renal Physiol* 300: F11–F23, 2011. doi:10.1152/ajprenal.00554.2010.
83. **Weiner ID, Verlander JW.** Ammonia transporters and their role in acid-base balance. *Physiol Rev* 97: 465–494, 2017. doi:10.1152/physrev.00011.2016.
84. **Weiner ID, Verlander JW.** Renal ammonia metabolism and transport. *Compr Physiol* 3: 201–220, 2013.
85. **Weiner ID, Verlander JW.** Ammonia transport in the kidney by Rhesus glycoproteins. *Am J Physiol Renal Physiol* 306: F1107–F1120, 2014. doi:10.1152/ajprenal.00013.2014.
86. **Xue Y, Liao SF, Son KW, Greenwood SL, McBride BW, Boling JA, Matthews JC.** Metabolic acidosis in sheep alters expression of renal and skeletal muscle amino acid enzymes and transporters. *J Anim Sci* 88: 707–717, 2010. doi:10.2527/jas.2009-2101.
87. **Yamada H, Yamazaki S, Moriyama N, Hara C, Horita S, Enomoto Y, Kudo A, Kawakami H, Tanaka Y, Fujita T, Seki G.** Localization of NBC-1 variants in human kidney and renal cell carcinoma. *Biochem Biophys Res Commun* 310: 1213–1218, 2003. doi:10.1016/j.bbrc.2003.09.147.
88. **Yamaguchi S, Ishikawa T.** AHCYL2 (long-IRBIT) as a potential regulator of the electrogenic Na(+)-HCO3(-) cotransporter NBCe1-B. *FEBS Lett* 588: 672–677, 2014. doi:10.1016/j.febslet.2013.12.036.
89. **Yang D, Shcheynikov N, Zeng W, Ohana E, So I, Ando H, Mizutani A, Mikoshiba K, Muallem S.** IRBIT coordinates epithelial fluid and HCO_3^- secretion by stimulating the transporters pNBC1 and CFTR in the murine pancreatic duct. *J Clin Invest* 119: 193–202, 2009.
90. **Yang SS, Fang YW, Tseng MH, Chu PY, Yu IS, Wu HC, Lin SW, Chau T, Uchida S, Sasaki S, Lin YF, Sytwu HK, Lin SH.** Phosphorylation regulates NCC stability and transporter activity in vivo. *J Am Soc Nephrol* 24: 1587–1597, 2013. doi:10.1681/ASN.2012070742.